Fisheries and Oceans Canada | Pêches et Océans Canada
Science | Sciences

C S A S | **S C C S**

Canadian Science Advisory Secretariat | **Secrétariat canadien de consultation scientifique**

Research Document 2003/044 | **Document de recherche 2003/044**

Not to be cited without
Permission of the authors *

Ne pas citer sans
autorisation des auteurs *

Environmental conditions in the Labrador Sea in Spring 2002

Conditions ambiantes dans la mer du Labrador au printemps 2002

R.M. Hendry, R.A. Clarke, J.R.N. Lazier, and/et I.M. Yashayaev

Department of Fisheries and Oceans, Maritimes Region
Ocean Sciences Division, Bedford Institute of Oceanography
P.O. Box 1006, Dartmouth, N.S. B2Y 4A2

* This series documents the scientific basis for the evaluation of fisheries resources in Canada. As such, it addresses the issues of the day in the time frames required and the documents it contains are not intended as definitive statements on the subjects addressed but rather as progress reports on ongoing investigations.

* La présente série documente les bases scientifiques des évaluations des ressources halieutiques du Canada. Elle traite des problèmes courants selon les échéanciers dictés. Les documents qu'elle contient ne doivent pas être considérés comme des énoncés définitifs sur les sujets traités, mais plutôt comme des rapports d'étape sur les études en cours.

Research documents are produced in the official language in which they are provided to the Secretariat.

Les documents de recherche sont publiés dans la langue officielle utilisée dans le manuscrit envoyé au Secrétariat.

This document is available on the Internet at:

Ce document est disponible sur l'Internet à:

http://www.dfo-mpo.gc.ca/csas/

ISSN 1499-3848 (Printed)
© Her Majesty the Queen in Right of Canada, 2003
© Sa majesté la Reine, Chef du Canada, 2003

Canada

ABSTRACT

The 2001-2002 winter over the Labrador Sea was more severe than the previous winter but still milder than normal. Observations in early-summer 2002 showed remnants of convective overturning to maximum depths of 1200-1400m, about 400m deeper than seen in the preceding two years. Apart from the apparent weak renewal of winter convection, the general trend was to warmer and more saline conditions. This was true both in the seasonally-active layer shallower than the maximum depth of convection and in the intermediate waters deeper than 1400m. The net result is that the 0-2000m early-summer mean salinity was the highest in the past thirteen years of regular observations. The corresponding mean temperature was the second highest observed during this period.

RÉSUMÉ

L'hiver 2001-2002 sur la mer du Labrador a été plus rigoureux que celui de l'année précédente, mais plus doux que la normale. Les observations faites au début de l'été 2002 ont révélé des renversements de convection résiduels jusqu'à des profondeurs maximales de 1200-1400 m, soit environ 400 m de plus que les deux années précédentes. Mis à part une faible reprise apparente de la convection hivernale, la tendance générale était vers des conditions plus chaudes et plus salines. Cette situation s'est avérée dans la couche active au niveau saisonnier qui est moins profonde que la profondeur maximale de la convection ainsi que dans les eaux intermédiaires de plus de 1400 m de profondeur. Le résultat net indique que la salinité moyenne du début de l'été, de 0 à 2000 m, a été la plus élevée depuis treize ans, période pendant laquelle les observations ont été régulières. La température moyenne correspondante était la deuxième plus élevée durant cette période.

INTRODUCTION

Hydrographic conditions in the Labrador Sea depend on a balance of atmospheric forcing, advection, and ice melt. Wintertime heat loss to the atmosphere in the central Labrador Sea is offset by warm waters carried northward by the offshore branch of the West Greenland Current. The excess salt carried by the warm inflows is balanced by other inflows of cold, fresh polar waters, fresh water from river runoff, and ice melt. Atmospheric forcing plays a relatively small role in the fresh water balance of the Labrador Sea compared with these advective effects.

Wintertime cooling and evaporation increase the density of surface waters in the central Labrador Sea. Wind mixing and vertical overturning form a mixed layer whose depth increases through the cooling season to some maximum value. The winter heat loss, the resulting density increase, and the depth to which the mixed layer penetrates vary with the severity of the winter. The density of the resulting mixed layer and the depth of convection also depend critically on the salinity of the waters exposed to the atmosphere. In extreme winters, mixed layers deeper than 2000 m have been observed. The intermediate-depth Labrador Sea Water formed by these extreme overturning events spreads throughout the northern North Atlantic. During milder years, the vertical stratification of temperature, salinity, and density is re-established.

Deep convection in the Labrador Sea provides an important pathway for atmospheric gases such as oxygen, carbon dioxide, and the chlorofluorocarbons (CFCs) to pass from the surface mixed layer to intermediate depths. As the convected Labrador Sea Water (LSW) flows to other regions of the ocean (Sy et al., 1997; Lavender et al., 2000), it distributes these dissolved gases to a large area of the ocean thereby ventilating the deeper layers. Because of the importance of this process and because of the large variability in the production rate of LSW, Ocean Sciences Division (Fisheries and Oceans Canada at the Bedford Institute of Oceanography) has occupied a line of CTD stations across the Labrador Sea in the early summer of each year since 1990. This line was designated line AR7W (Atlantic Repeat Hydrography Line 7 West) during the World Ocean Circulation Experiment (WOCE). Between 1990 and 1997 the work was a contribution to WOCE. Since 1997, the work has continued as a Canadian contribution to the North Atlantic Oscillation and the Atlantic Thermohaline Circulation Principal Research Areas of the Climate Variability and Predictability (CLIVAR) project of the World Climate Research Programme (WCRP).

This report summarises the results of a transect of AR7W on CCGS Hudson Expedition 2002-032, June 23 - July 18, 2002. This transect was part of a broader program in physical, biological, and chemical oceanography within the Northwest Atlantic and Labrador Sea under the scientific direction of Chief Scientist R. Allyn Clarke.

Figure 1 shows a map of the Labrador Sea with station positions for 2002-032, including 101 full-depth CTD stations using a Sea-Bird Electronics, Inc. 911*plus* CTD system for temperature, salinity, and oxygen. Rosette bottle samples provided point measurements of oxygen, nutrients, and other biological and chemical parameters.

Also shown in Figure 1 are the Bravo mooring site in the central Labrador Sea near the historical location of Ocean Weather Ship Bravo and ground tracks of the TOPEX/POSEIDON altimetric satellite.

ATMOSPHERIC FORCING

Monthly-averaged air-sea flux fields produced by the co-operative Reanalysis Project (Kistler et al., 2001) of the U.S. National Centers for Environmental Prediction (NCEP) and National Center for Atmospheric Research (NCAR) were used to estimate air-sea exchanges of heat for the period January 1948 to November 2002. The heat fluxes discussed here are sums of NCEP net short wave radiation flux, net long wave radiation flux, sensible heat flux, and latent heat flux. The monthly-averaged NCEP fields were obtained from the NOAA-CIRES Climate Diagnostics Center web site http://www.cdc.noaa.gov/. The grid point at 56.2°N, 52.5°W marked in Figure 1 is about 40 km south of the nearest AR7W station. The fields at this grid point represent an area approximately 115 km in east-west extent and 210 km in north-south extent.

Twelve-month June - May averages of heat flux (centred on the winter cooling season) over the past 15 years are shown in Figure 2(a). A positive heat flux indicates a loss of heat from the ocean to the overlying atmosphere. A 30-year period is considered long enough to calculate a representative average to define so-called normal conditions. The period 1961-1990 is widely used but many agencies are shifting to 1971-2000. The mean NCEP heat flux in the central Labrador Sea for the 30-year period 1961-1990 was 60 $W \cdot m^{-2}$. Winters in the early years of the 1990's were quite severe; the mean NCEP heat flux for the same location for the 1971-2000 30-year period was 66 $W \cdot m^{-2}$, 10 percent greater than for the earlier 30-year period. Because we are interested in seasonal means, we chose the 31-year normal period June 1970 - May 2001 to allow for averages over the same number of cases for each season. The mean heat flux over this 31-year period is 65 $W \cdot m^{-2}$. The mean heat flux for June 2001 - May 2002 leading up to the 2002 occupation of AR7W was 51 $W \cdot m^{-2}$, 14 $W \cdot m^{-2}$ less than the mean for the 31-year normal period. The 2001-2002 mean heat flux falls at the 26th percentile of the frequency distribution of 12-month mean heat fluxes for the 31-year normal period. However, the 2001-2002 winter was more severe than the preceding one: the mean heat flux for June 2000 - May 2001 was 32 $W \cdot m^{-2}$, tied with the June 1995 - May 1996 average for the lowest in the 31-year normal period.

Seasonal heat fluxes for the past three years are shown in Figure 2(b). The seasons are defined as Summer = June-August, Fall = September-November, Winter = December-February, and Spring = March-May. For the year leading up to the 2002 AR7W occupation, the winter average heat flux was 60 $W \cdot m^{-2}$ less than normal (16th percentile) while summer, fall, and spring averages were near normal. Similarly low heat fluxes in the winter season for the 2000-2001 period winter (17th percentile) were combined with a record-low 2000-2001 average spring heat flux to produce an overall low 12-month mean for 2000-2001.

RESULTS FROM 2002

Property distributions in 2002

Contoured gridded sections of potential temperature, salinity, potential density anomaly, potential vorticity, and apparent oxygen utilisation (AOU) for the 2002 AR7W occupation are shown in Figures 3-7. Along-section distance in kilometres increasing from west to east is used as the horizontal coordinate. Each upper-panel section plot uses depth as the vertical coordinate. The corresponding plot in the lower panel uses potential density anomaly as the vertical coordinate. An attempt is made to exclude the seasonally-active layer from the plots using potential density anomaly as vertical coordinate by treating only potential density anomalies greater than 27.7 $kg \cdot m^{-3}$. The mean depth of the 27.7 $kg \cdot m^{-3}$ potential density anomaly surface is 269 m, with extreme depths of 156 m and 753 m.

Notable in the near-surface levels of Figure 3(a) (potential temperature) are cold waters (<2°C) over the Labrador Shelf on the western boundary of the Labrador Sea. The shelf waters are separated from the interior by a shelf-break front associated with the southward flowing Labrador Current. Similarly cold waters in the upper few hundred metres at the eastern boundary of the Labrador Sea are bounded to the west by another frontal region associated with the inshore branch of the northward-flowing West Greenland Current. Warmer waters (>4°C) in the upper 500 m of the water column near the eastern boundary are associated with the offshore branch of the West Greenland Current. A maximum surface temperature of about 6.6°C and an associated seasonal thermocline were observed in the July 2002 survey.

Figure 3(a) shows a large area of LSW between 600 m and 1200 m in the central Labrador Sea with potential temperature less than 3.2°C and reduced vertical temperature gradients, especially for the western half of the section. Just below the LSW is found a quasi-continuous layer with potential temperature greater than 3.3°C. This relatively warm layer originates at the eastern boundary near 1300 m depths. It deepens to 1500 m at its western limit before finally disappearing near the 300-km mark. At still deeper levels, potential temperature decreases with depth to near-bottom values less than 2°C. The prominent slopes of the deep isotherms near the western and eastern boundaries are associated with the deep boundary current that circles the Labrador Sea in a counterclockwise sense.

Figure 3(b) shows that potential temperature is nearly constant on surfaces of constant potential density except at the uppermost levels. Mesoscale eddy features that distort the property fields on surfaces of constant depth have less influence on the distribution of properties on surfaces of constant potential density. For this reason, year-to-year changes in the property fields may be seen more clearly in density space.

We interpret the relative minimum in potential temperature as a remnant of convective formation of LSW that took place during the 2001-2002 winter. In early July 2002 the waters shallower than about 250 m depth will have warmed considerably from their

winter conditions because of heating from the atmosphere (Appendix A). The warming of the waters above the relative minimum in potential temperature but deeper than say 250 m cannot be explained by direct atmospheric forcing. This warming can be attributed to horizontal/isopycnal advection and mixing, possibly accompanied by secondary vertical/diapycnal mixing. The upper of the pair of dashed lines superimposed on each of Figures 3(a) and 3(b) traces the depth or potential density anomaly respectively of the relative minimum in potential temperature. The area enclosed by the 3.2°C potential temperature contour at mid-depths is greater near the western side of the Labrador Sea than the eastern side. The minimum potential temperature layer occurs at somewhat greater depths and greater potential densities on the western side than on the eastern side. This is compatible with the notion that winter convection occurs predominantly on the western side of the Labrador Sea, driven by outbreaks of cold, dry air from the north and west (Clarke and Gascard, 1983).

We interpret the relative maximum in potential temperature near 1400 m as the signature of nearly-isopycnal spreading of relatively warm and saline waters from the eastern boundary of the Labrador Sea. The lower of the pair of dashed lines superimposed on each of Figures 3(a) and 3(b) traces the depth or potential density anomaly respectively of the relative maximum in potential temperature.

The patch with salinity less than 34.88 near 2000 m depth or 27.78 $kg \cdot m^{-3}$ potential density anomaly in Figures 4(a) and 4(b) respectively is a remnant of Deeper LSW formed by deep convection in a series of severe winters between 1988 and 1993 (Lazier et al., 2002). Salinities greater than 34.9 near 3000 m depth or 27.85 $kg \cdot m^{-3}$ potential density anomaly mark the influence of Northeast Atlantic Deep Water that enters the North Atlantic from the Nordic Seas via the Faroe - Shetland overflows (Hansen and Østerhus, 2000).

Figure 5(a) shows potential density anomaly on pressure surfaces and Figure 5(b) shows pressure on potential density anomaly surfaces. The unit of pressure is the decibar (dbar). The numerical value of depth in metres is approximately the same as the numerical value of pressure in decibars.

Figure 6 (potential vorticity) shows a local minimum in potential vorticity that closely follows the relative minimum in potential temperature. There is a layer of relatively high potential vorticity near or just below the potential temperature maximum. Still deeper in the water column near 2000 m depth and 27.78 $kg \cdot m^{-3}$ potential density anomaly there is another potential vorticity minimum related to the Deeper LSW discussed above.

Figure 7 shows apparent oxygen utilisation (AOU) derived from bottle samples. AOU is defined as the difference between the saturation value of dissolved oxygen concentration at the measured temperature and salinity and the measured dissolved oxygen concentration. It provides a measure of the time elapsed since the water was in contact with the atmosphere, since biological processes tend to reduce oxygen concentration with time. The waters between the seasonally-heated top few hundred metres and the potential temperature minimum show nearly constant AOU values of

about 0.6 $mL \cdot L^{-1}$. Higher values of AOU are observed below the potential temperature minimum, marking waters that have been out of contact with the atmosphere for a longer period of time. The Deeper LSW shows up as a relative minimum in AOU.

CHANGES IN PROPERTIES FROM EARLIER YEARS

Sections showing changes from 2001 to 2002

Contoured gridded sections of the changes in potential temperature, salinity, potential density anomaly or pressure on potential density surfaces, potential vorticity, and AOU from the 2001 to the 2002 AR7W occupations are shown in Figures 8-12. Pairs of plots with depth as the vertical coordinate in the upper panel and potential density anomaly as the vertical coordinate in the lower panel are presented as in Figures 2-7. Figure 10 shows changes in potential density on pressure surfaces in the upper panel and change in pressure on potential density anomaly surfaces in the lower panel.

The changes in the upper 200 m are dominated by seasonal effects. The 2001 occupation took place in early June. The 2002 occupation took place in early July, one month later in the seasonal cycle.

The depths of relative minima and maxima in potential temperature for 2002 are superimposed on the difference sections as in Figures 2-7. The depths of similar minima and maxima in potential temperature for the 2001 occupation are also marked. In the western part of the transect, the relative minima and maxima in potential temperature for 2002 occur deeper in the water column than was the case in 2001.

In summary, there is a generally horizontally-coherent layered pattern of property changes. The upper 1000 m became warmer, saltier and slightly denser; a layer centred near the 1000 m mark in the western two-thirds of the basin became colder and fresher without much change in density; and the waters deeper than this freshening layer became warmer, saltier, and slightly less dense.

Changes in the 0-1000 m layer

Figures 8(a) and 8(b) (potential temperature change) show a general warming of 0.1-0.2°C over much of the water column above the 1000 m level. The changes in temperature on surfaces of constant pressure include the effects of transient mesoscale eddies. The warming is seen more clearly on potential density surfaces in Figure 8(b). Figure 9 shows that this layer also became saltier between 2001 and 2002. Figure 10(a) shows that the salinity increase dominated the temperature increase in terms of density changes: the density of this upper layer increased slightly. Figure 10(b) shows an equivalent shallowing of pressure surfaces by several hundred metres. Figure 11 suggests an increase in the vertical density stratification in the 0-500 m range and a decrease in the 500-1000 m range. All these changes are consistent with a greater

influence in 2002 than in 2001 of the warm and salty waters originating in the warm branch of the West Greenland Current.

Changes near 1000m

Figures 8(a) and 8(b) show a pronounced cooling of a layer extending from about 800 m to 1200 m depths over the western two-thirds of the basin. Figure 9 shows that this layer was also fresher in 2002 than in 2001. There is no clear pattern of density change in this layer. However, Figures 11 and 12 show that this layer experienced a decrease in potential vorticity and AOU (increase in dissolved oxygen) from 2001 to 2002. This is consistent with the idea that there was deeper vertical convection in the winter of 2001-2002 than in the preceding winter.

Changes in the 1000-2000 m layer

Figures 8(a) and 8(b) show a remarkable warming of the deeper waters of the Labrador Sea between 2001 and 2002. The changes are greatest in the 1500-2000 m depth range below the LSW influence: the waters in this depth range are also notably saltier in 2002 than in 2001. The density changes on pressure surfaces or the equivalent pressure changes on density surfaces are directly affected by mesoscale transients and are less spatially coherent. There is a general decrease in density, increase in potential vorticity, and increase in AOU in the 1500-2000 m range on the western half of the transect. As in the uppermost layer, this suggests a greater influence of waters originating on the eastern boundary. Present estimates of the transit time for waters from the eastern boundary to circulate around the Labrador Sea to the western boundary are of order one year.

Average profiles from 2002, 2001, and 2000

The vertical structure in potential temperature in 2002 may be seen more clearly in Figures 13(a) and 13(b), which show individual profiles of potential temperature for the 11 stations in the distance range 240-700 km. The vertical coordinates are pressure in the range 200-2000 dbar and potential density anomaly in the range 27.7-27.8 $kg \cdot m^{-3}$ respectively. The mean depth of the 27.8 $kg \cdot m^{-3}$ potential density anomaly surface is 2163 m, with extremes of 1663 m and 2329 m. An average profile and selected standard deviations are also shown. There is less scatter on potential density surfaces than on pressure surfaces; this is reflected in the smaller standard deviations in Figure 13(b) compared with Figure 13(b). Similar averages in the 240-700 km distance range for 2000 and 2001 are included for comparison.

The 2002 average in Figure 13(a) shows a broad relative minimum in potential temperature with values of about 3.15°C centred near 1000 dbar. The averages from the two preceding years show weaker relative minima centred at 800 dbar for 2000 and 900 dbar for 2001. The 2002 average shows a well-defined relative maximum potential temperature of 3.27°C centred near 1500 dbar. The averages from the two preceding

years show somewhat shallower relative maxima, centred near 1100 dbar for 2000 and 1150 dbar for 2001.

The 2002 average on potential density surfaces in Figure 13(b) shows a relative minimum in potential temperature centred at 27.74 $kg \cdot m^{-3}$, slightly higher than the 27.73 $kg \cdot m^{-3}$ value corresponding to the relative minima for the average profiles from the preceding two years. Relative maxima in the average potential temperature profiles appear at 27.76 $kg \cdot m^{-3}$ potential density anomaly for 2002 and at 27.755 $kg \cdot m^{-3}$ for the previous two years.

Figures 14(a) and 14(b) show similar averages of AOU. The 800-1200 m layer shows a decrease in AOU in 2002 relative to the previous two years. This supports the idea that this water was exposed to the atmosphere during the 2001-2002 winter.

Changes in heat and salt content 1990-2002

The changes in heat and salt for the 1990-2000 period were discussed by Lazier et al. (2002). This section extends the time series in Lazier et al. (2002) to include two additional AR7W occupations.

Figure 15(a) shows the heat content from spring AR7W occupations averaged over stations in the distance range 320-520 km as a function of median station date. Integrals over the depth ranges 150-1000 m and 1000-2000 m and the sum over these two depth ranges are shown. The units are $GJ \cdot m^{-2}$. A warming of a column of water 1850 m thick (i.e. 150-2000 m) by 0.13°C gives an increase in heat content of about 1 $GJ \cdot m^{-2}$. Figure 15(b) shows a similar plot of salt content. The units are $kg \cdot m^{-2}$. A salinity increase of about 0.005 for the same case gives an increase in salt content of about 10 $kg \cdot m^{-2}$.

The heat content in the 150-1000 m layer remained greater than the 13-year mean in 2002, increasing from the preceding two years. The salt content of this layer in 2002 was slightly greater than the mean, following two years of below-average values. The high-frequency variability in 150-1000 m salt content was noted by Lazier et al. (2002).

Increasing trends in heat and salt content in the 1000-2000 m layer were noted by Lazier et al. (2002). Both trends continued through 2001. In 2002, the heat content continued to increase but the salt content decreased by 2 $kg \cdot m^{-2}$ compared with 2001. The slight decrease in salt content of this layer was the net result of a 7 $kg \cdot m^{-2}$ decrease in the 1000-1500 m depth range associated with the increased presence of relatively-fresh LSW and a 5 $kg \cdot m^{-2}$ increase in the 1500-2000 m depth range. The 1000-2000 m average salt content was still the second highest of the 13-year record. The 1500-2000 m average salt content was the highest observed in the 13-year record.

The net result is that the 150-2000 m early-summer 2002 mean salinity was the highest observed in the past thirteen spring-summer periods for which measurements are available. The corresponding mean temperature was the second highest observed

during this period. The density of seawater decreases with increasing temperature and increases with increasing salinity. The 2002 survey showed slightly denser waters in the 150-1000 m depth range and slightly less-dense waters in the 1000-2000 m depth range compared with results from 2001. The net effect was a small decrease in 150-2000 m mean density, equivalent to a rise in steric sea level of the order 0.01 m.

There is a strong seasonal signal in the properties in the 0-150 m layer. Appendix A summarises an analysis of the seasonal cycle in the central Labrador Sea from historical data.

SEA LEVEL CHANGES FROM TOPEX/POSEIDON ALTIMETRY AND HYDROGRAPHY

Time series of sea level in the central Labrador Sea near the Bravo mooring site (Figure 1) were extracted from TOPEX/POSEIDON (T/P) Maps of Sea Level Anomaly (MSLA) altimeter data products produced by the French Archivage, Validation et Interprétation des données des Satellites Océanographiques (AVISO) (http://www-aviso.cls.fr/). Data were available for the period October 1992 through February 2002. A seasonal signal was estimated by a least-squares fit to annual and semiannual harmonics and the residuals were low-pass filtered. Additional data from the nearby crossover point of T/P Tracks 098 and 243 referred to the same datum were treated in a similar way to extend the time series to August 11, 2002. Shortly after this date, the T/P orbit was changed to begin a combined mission with the Jason-1 satellite.

Figure 16 shows time series of low-passed altimetric sea level with and without the seasonal signal. The seasonal signal has a range of just less than 0.09 m. Also shown are time changes in geopotential height relative to 2000 dbar calculated from AR7W measurements since 1990 relative to the mean of Spring values during the T/P measurement period. Each value is an average of approximately four stations in the 320-520 km distance range. Standard deviations for each cruise are also shown. There is reasonable agreement between the changes in geopotential height relative to 2000 dbar and the changes in sea-level measured by T/P. This holds true for the changes from 2001 to 2002. Both the 0-2000 dbar geopotential heights and the low-frequency sea level time series show an increase of 0.01-0.02 m between the 2001 and 2002 AR7W occupations.

SUMMARY

Since the winter of 1994-1995, mild winters have produced wintertime convection in the Labrador Sea to maximum depth of order 1000 m, compared with depths greater than 2000 m in the early 1990's. This pattern persisted through the winter of 2001-2002. Annual sea-air heat fluxes (June 2001 - May 2002) in the central Labrador Sea estimated from the NCEP/NCAR Reanalysis Project were about 14 $W \cdot m^{-2}$ less than normal, defined as the mean over the 31-year period June 1970 - May 2001. The 2001-

2002 12-month average fell in the 26th percentile of cases for this period. Wintertime (December-February) heat fluxes were nearly 60 W·m^{-2} less than normal. However, the 2001-2002 winter was more severe than the 2000-2001 winter.

A July 2002 transect of the Labrador Sea showed evidence of vertical overturning during the previous winter to depths of 1200-1400 m. This evidence consisted of subsurface remnants of a presumed wintertime surface mixed-layer with high dissolved oxygen, relative minimum potential temperature, and reduced vertical density stratification. The inferred winter mixed layer had a characteristic potential temperature of 3.15°C, a salinity of 34.83, and a potential density anomaly of 27.74 kg·m^{-3}. In contrast, the deep mixed layers observed in the early 1990's had potential density anomalies near 27.78 kg·m^{-3}.

Apart from the apparent weak renewal of winter convection and an associated cooling and freshening near 1000 m, the general trend was to warmer and more saline conditions. This was true both in the layer shallower than the inferred maximum depth of convection and in the intermediate waters deeper than 1400 m.

The 150-1000 m mean temperature in the central Labrador Sea was the second highest observed in the thirteen-year period of annual surveys, surpassed only by 1999. The salinity of the upper 1000 m was greater than observed since the period of deep convection of the early 1990's. The increase in heat and salt of the upper layers of the Labrador implies a greater influence of warm, saline waters carried north into the Labrador Sea by the offshore branch of the West Greenland Current. The high salinities observed in the early 1990's resulted from a different mechanism, the vertical entrainment of higher-salinity waters from deeper levels into the upper ocean as a result of convection deeper than 1000 m.

Since the mid-1990's, a notable trend to higher temperature and salinity in the 1000-2000 m layer has emerged. In spite of the effects of somewhat increased winter overturning noted above, the mean temperature of this layer in early-summer 2002 was the warmest observed at comparable seasonal times during the past thirteen years. Salinity averaged over this depth range showed a slight decrease from the record-high conditions of the previous year. A continuing increase in the average salinity of the the1500-2000 m depth range was overcome in the 1000-2000 m average by the arrival of fresher LSW in the 1000-1500 m depth range.

The net result is that the mean 150-2000 m early-summer 2002 salinity was the highest observed in the past thirteen spring-summer periods for which measurements are available. The corresponding mean temperature was the second highest observed during this period. The density of seawater decreases with increasing temperature and increases with increasing salinity. The 2002 survey showed slightly denser waters in the 150-1000 m depth range and slightly less-dense waters in the 1000-2000 m depth range compared with results from 2001. The net effect was a small decrease in 150-2000 m mean density, equivalent to a rise in steric sea level of the order 0.01 m. Sea

level changes measured by the TOPEX/POSEIDON altimetric satellite are consistent with this result.

ACKNOWLEDGMENTS

This study was partially funded by the Ocean Climate Program of the Canadian Department of Fisheries and Oceans Science Strategic Fund. The altimeter products used were produced by French AVISO/Altimetry operations centre. The MSLA products were produced by the CLS Space Oceanography Division as part of the European Union Environment and Climate project AGORA (ENV4-CT9560113) and DUACS (ENV4-CT96-0357) with financial support from the CEO programme (Centre for Earth Observation) and Midi-Pyrénées regional council.

APPENDIX A

Annual variability in the central Labrador Sea from OWS Bravo

Temperature and salinity in the upper layers of the Labrador Sea undergo a marked annual cycle (Lazier, 1980). The annual AR7W surveys do not take place at exactly the same time each year, leading to some aliasing of the seasonal changes. To quantify these effects, annual cycles of temperature, salinity, and associated derived parameters in the upper 150 m of the central Labrador Sea were estimated by revisiting the hydrographic data from Ocean Weather Ship (OWS) Bravo located at 56.5°N, 51°W discussed in detail by Lazier (1980).

The four-year period from January 1964 to December 1967 showed a relatively stationary seasonal cycle. For this period, potential temperature averaged over 0-150 m varied annually from an overall mean of 4.3°C by ±1°C with a minimum in late-February and a maximum in mid-September (Figure A1). During the same period, salinity averaged over 0-150 m varied annually from an overall mean of 34.75 by ±0.06 with a minimum in early May and a maximum in mid-November (Figure A2). Potential density anomaly averaged over 0-150 m varied annually from an overall mean of 27.55 $kg \cdot m^{-3}$ by ±0.2 $kg \cdot m^{-3}$ with a maximum in early April and a minimum in mid-September. Steric sea level (Figure A3) varied annually by ±0.025 m. Minimum sea level corresponds to maximum potential density anomaly and vice versa. Density or steric sea level changes related to temperature variability were a factor of three greater than the changes related to salinity variability.

The changes in measured fields between the 2001 and 2002 early-summer occupations of AR7W can be estimated from the OWS Bravo results. The median date of the 2001 survey was June 6 and the median date of the 2002 survey was July 5, for a 29-day difference. The warming trend during the late spring and early summer would give a change of 0.5°C in 0-150 m average temperature using the 1964-1967 annual cycle. This is equivalent to 0.3 $GJ \cdot m^{-2}$ heat content. The decreasing trend in upper-layer

salinity would give a change of -0.02, equivalent to -3 $kg \cdot m^{-2}$ salt. The increasing trend in steric sea level would give a change of about 0.01 m.

As a check on the sensitivity of the annual cycle to the measurement period a similar calculation was carried out for the two-year period June 1972 to May 1974 which showed more salinity variability and greater wintertime heat loss than the earlier period (Lazier, 1980). The 0-150 m layer was colder by 0.9 °C, fresher by 0.14, and less dense by 0.02 $kg \cdot m^{-3}$ during this period than for the 1964-1967 period. The annual cycles for this period are also shown in Figures A1, A2, and A3. The temperature cycle is comparable to the results from the earlier period but the salinity cycle has double the range and noticeably different phasing compared with the 1964-1967 result. It gives a salinity change of -0.05, equivalent to -8 $kg \cdot m^{-2}$ salt, for the 29-day June-July interval. Since density changes are dominated by temperature changes, the annual cycles in steric sea level for the two periods are similar.

REFERENCES

Clarke, R.A. and J.-C. Gascard. 1983. The formation of Labrador Sea Water. Part I: Large-scale processes. Journal of Physical Oceanography, 13: 1764-1788.

Hansen, B. and S. Østerhus. 2000. North Atlantic - Nordic Seas Exchanges. Progress in Oceanography, 45: 109-208.

Kistler, R., E. Kalnay, W. Collins, S. Saha, G. White, J. Woollen, M. Chelliah, W. Ebisuzaki, M. Kanamitsu, V. Kousky, H. van den Dool, R. Jenne, and M. Fiorino. 2001. The NCEP-NCAR 50-Year Reanalysis: Monthly Means CD-ROM and Documentation. Bulletin of the American Meteorological Society, 82: 247-268.

Lavender, K.L., R.E. Davis, and W.B. Owens. 2000. Mid-depth recirculation observed in the interior Labrador and Irminger Seas by direct velocity measurements. Nature, 407: 66-69.

Lazier, J.R.N. 1980. Oceanographic conditions at Ocean Weather Ship Bravo, 1964-1974. Atmosphere-Ocean, 18: 227-238.

Lazier, J., R. Hendry, A. Clarke, I. Yashayaev, and P. Rhines. 2002. Convection and restratification in the Labrador Sea, 1990-2000. Deep-Sea Research I, 49: 1819-1835.

Sy, A., M. Rhein, J.R.N. Lazier, K.P. Koltermann, J. Meincke, A. Putzka, and M. Bersch. 1997. Surprisingly rapid spreading of newly formed intermediate waters across the North Atlantic Ocean. Nature, 386: 675-679.

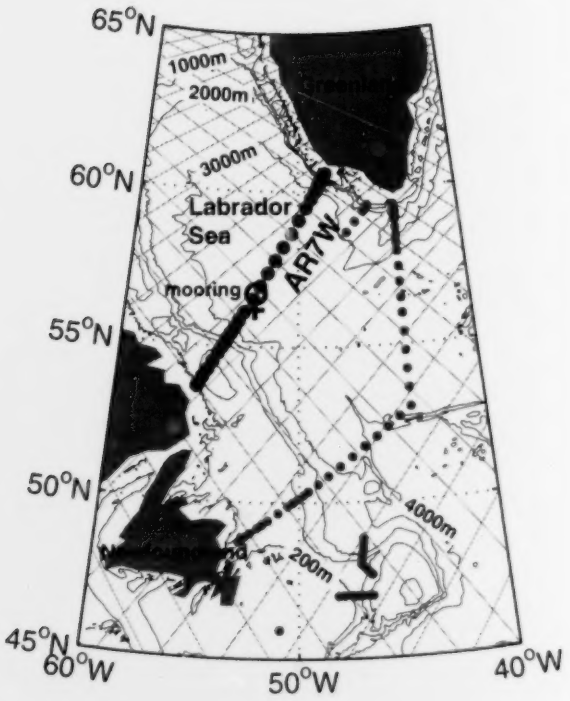

Fig. 1 Map of the Labrador Sea showing CTD station positions for Hudson Expedition 2002-032 (large circles - AR7W stations; small circles - additional stations). The Bravo mooring site is marked with an open circle. A nearby NCEP/NCAR Reanalysis grid point referred to in the text is marked with a cross. TOPEX/POSEIDON ground tracks and selected bathymetric contours are also shown.

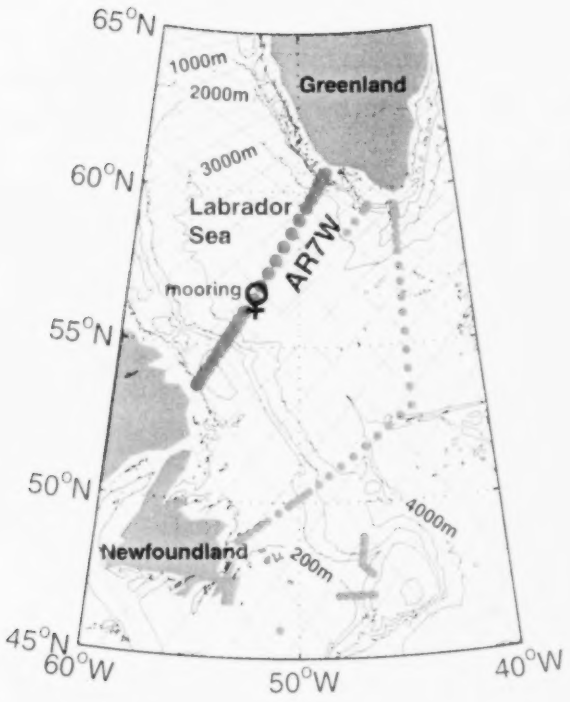

Fig. 1 Map of the Labrador Sea showing CTD station positions for Hudson Expedition 2002-032 (large circles - AR7W stations, small circles - additional stations). The Bravo mooring site is marked with an open circle. A nearby NCEP/NCAR Reanalysis grid point referred to in the text is marked with a cross. TOPEX/POSEIDON ground tracks and selected bathymetric contours are also shown.

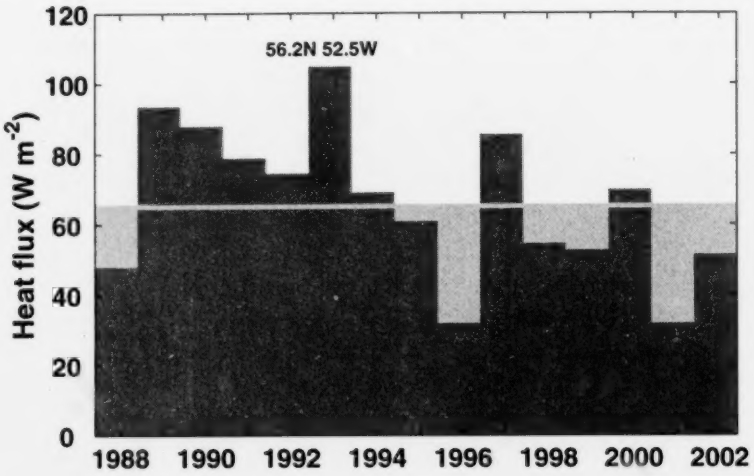

Fig. 2(a) 12-month averages (June-May) of monthly-mean NCEP sea-air heat flux at 56.2°N, 52.5°W in the central Labrador Sea. Values within the shaded area are lower than the mean (65 $W \cdot m^{-2}$) for the normal period June 1970 - May 2001. Values for the most-recent two 12-month periods were lower than normal: 51 $W \cdot m^{-2}$ (26th percentile) for June 2001 - May 2002 and a near-record low of 32 $W \cdot m^{-2}$ for June 2000 - May 2001.

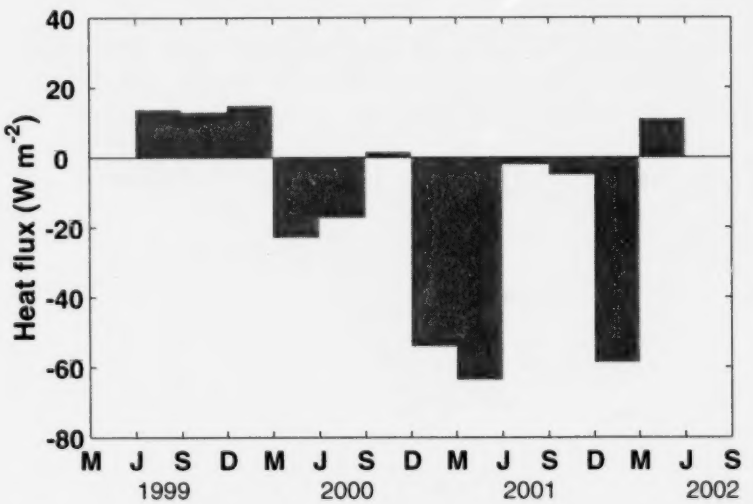

Fig. 2(b) Seasonal averages (summer = JJA, fall = SON, winter = DJF, spring = MAM) of monthly-mean NCEP sea-air heat flux anomalies at 56.2°N, 52.5°W in the central Labrador Sea for the period Summer 1999 - Spring 2002. The anomalies are relative to seasonal means for the normal period June 1970 - May 2001. For 2001-2002, the winter average heat flux was less than normal (16th percentile). Summer, fall, and spring averages were near normal. For 2000-2001, both winter (17th percentile) and spring (0th percentile) fluxes were less than normal.

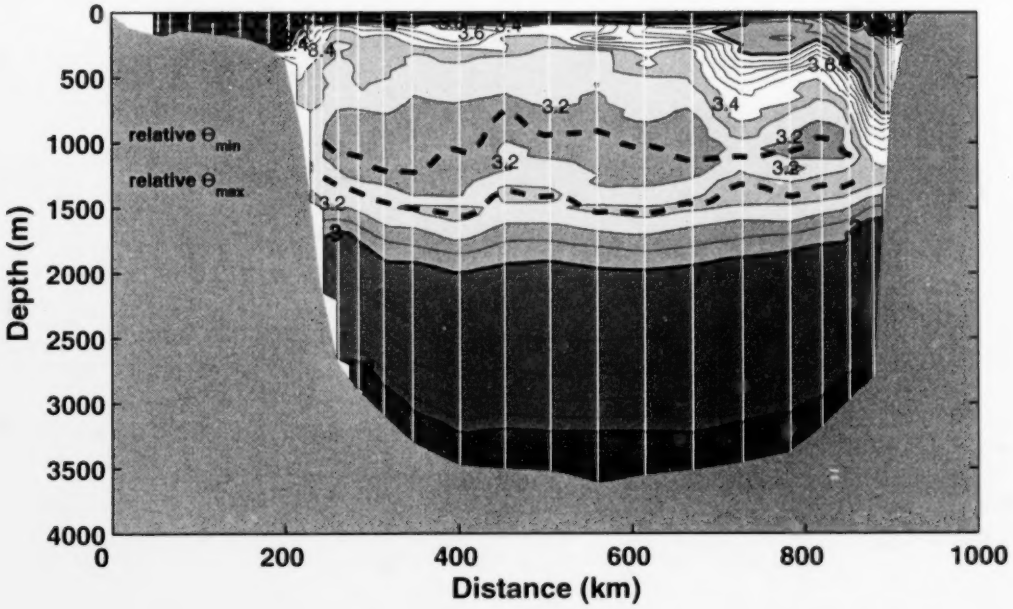

Fig. 3(a) Potential temperature (°C) on AR7W during July 2-9, 2002, from Hudson 2002-032. The dashed lines trace layers of relative minimum potential temperature (< 3.2°C) and relative maximum potential temperature (generally >3.3°C).

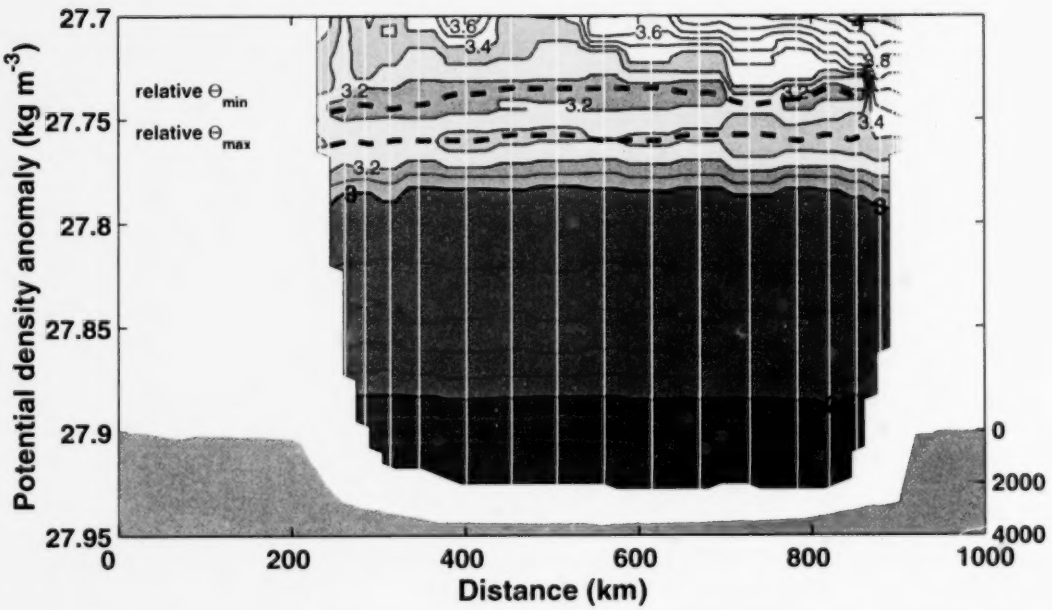

Fig. 3(b) Potential temperature (°C) on AR7W using potential density anomaly as the vertical coordinate for potential density anomalies greater than 27.7 kg·m^{-3} during July 2-9, 2002, from Hudson 2002-032. The dashed lines trace layers of relative minimum and maximum potential temperature as in Figure 3(a). An overlay shows the section bathymetry (m). The scale for the bathymetry is at lower right.

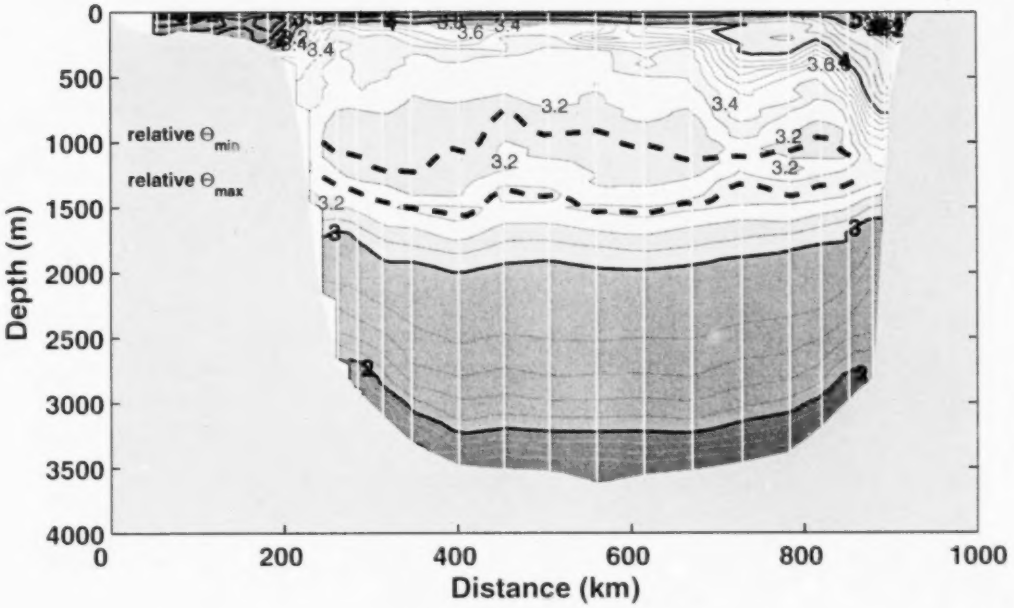

Fig. 3(a) Potential temperature (°C) on AR7W during July 2-9, 2002, from Hudson 2002-032. The dashed lines trace layers of relative minimum potential temperature (< 3.2°C) and relative maximum potential temperature (generally >3.3°C).

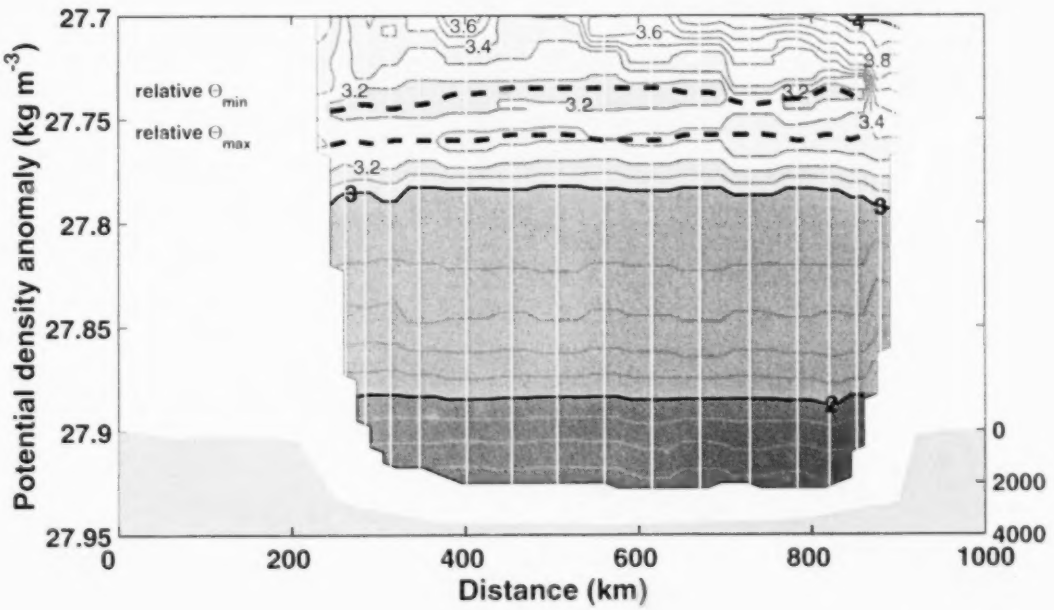

Fig. 3(b) Potential temperature (°C) on AR7W using potential density anomaly as the vertical coordinate for potential density anomalies greater than 27.7 kg·m^{-3} during July 2-9, 2002, from Hudson 2002-032. The dashed lines trace layers of relative minimum and maximum potential temperature as in Figure 3(a). An overlay shows the section bathymetry (m). The scale for the bathymetry is at lower right.

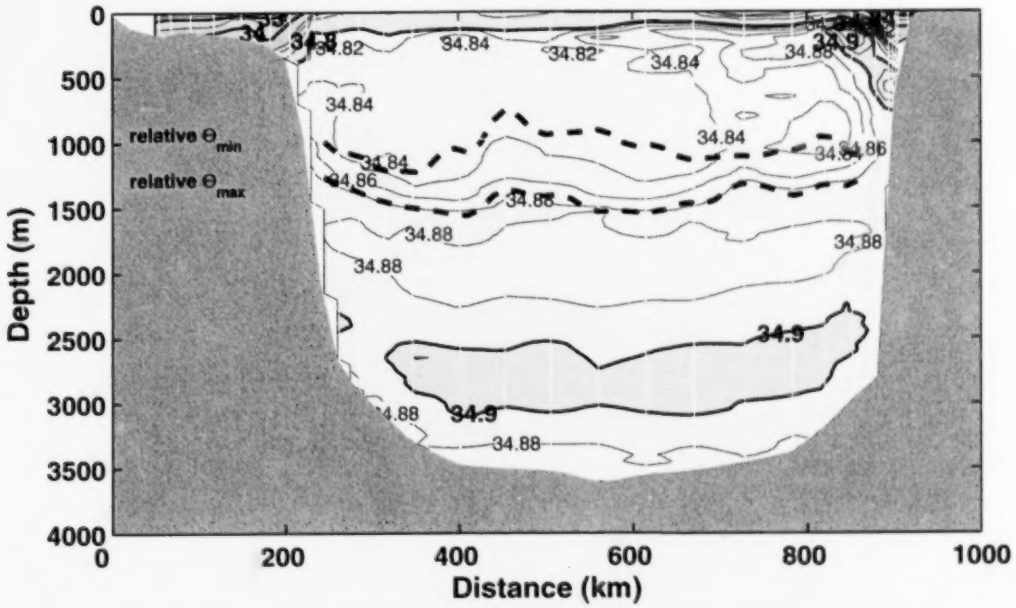

Fig. 4(a) Salinity on AR7W during July 2-9, 2002, from Hudson 2002-032. The dashed lines trace layers of relative minimum potential temperature and relative maximum potential temperature as in Figure 3(a).

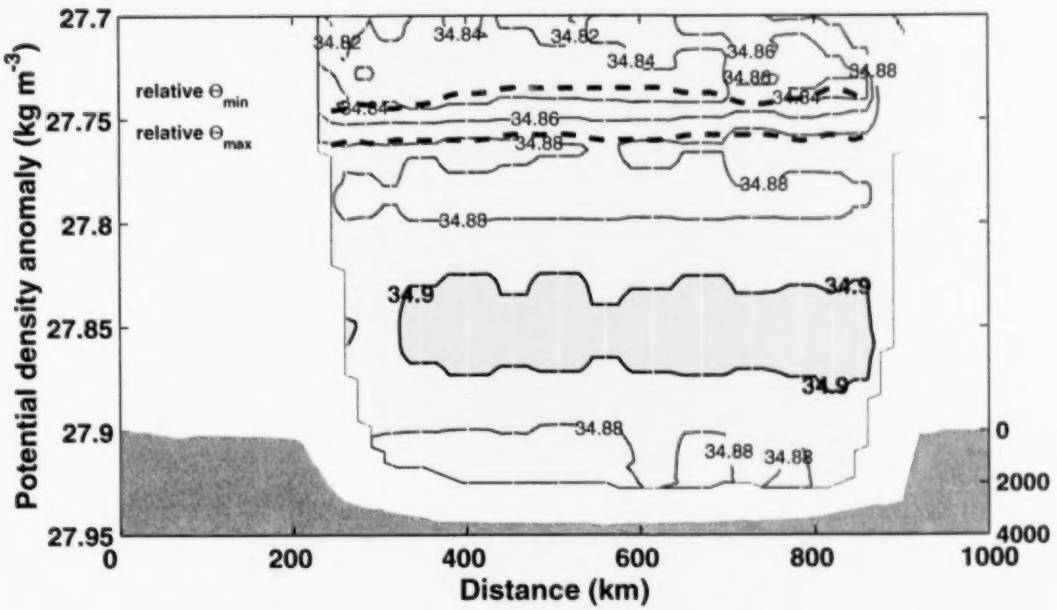

Fig. 4(b) Salinity on AR7W using potential density anomaly as the vertical coordinate for potential density anomalies greater than 27.7 kg·m^{-3} during July 2-9, 2002, from Hudson 2002-032 as in Figure 3(b).

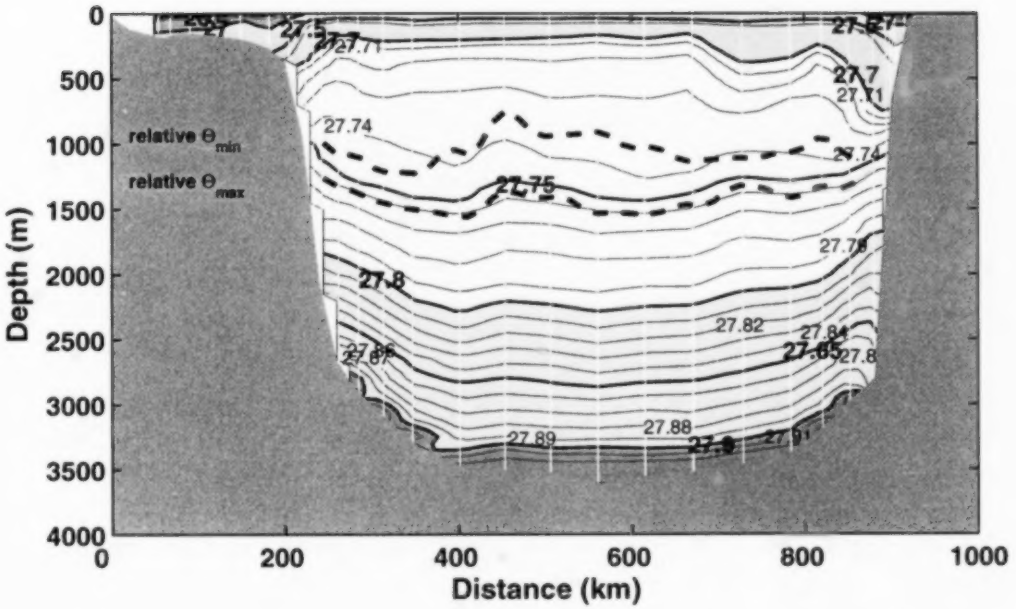

Fig. 5(a) Potential density anomaly (kg·m^{-3}) on AR7W during July 2-9, 2002, from Hudson 2002-032. The dashed lines trace layers of relative minimum potential temperature and relative maximum potential temperature as in Figure 3(a).

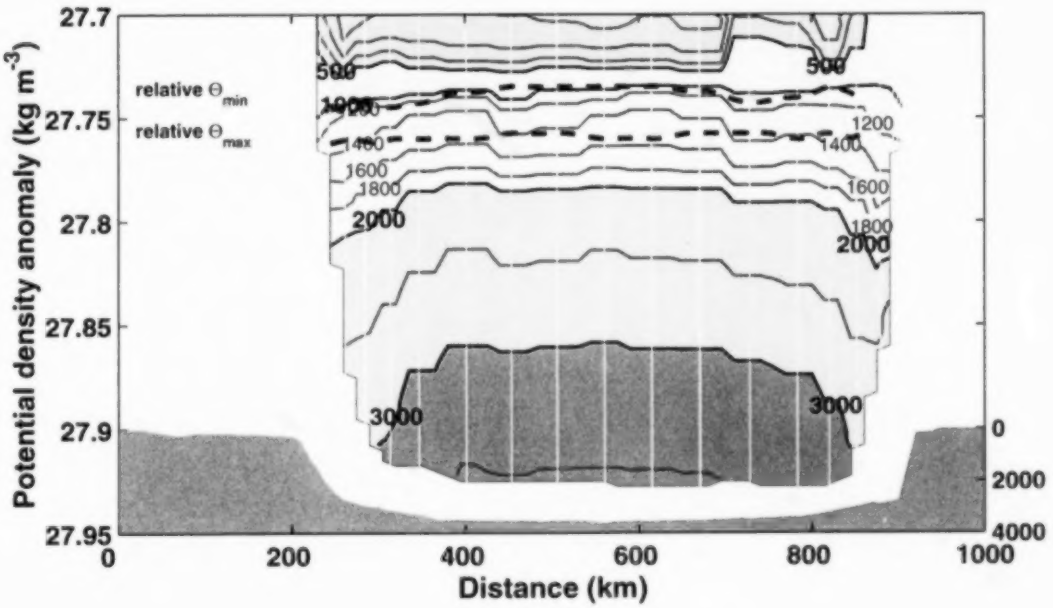

Fig. 5(b) Pressure (decibars) on AR7W using potential density anomaly as the vertical coordinate for potential density anomalies greater than 27.7 kg·m^{-3} during July 2-9, 2002, from Hudson 2002-032 as in Figure 3(b).

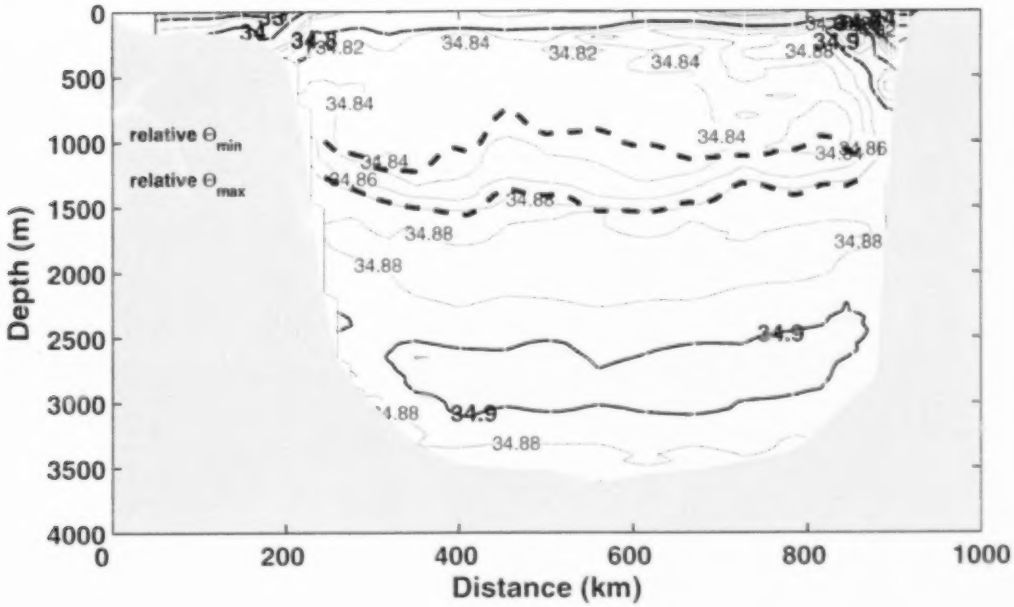

Fig. 4(a) Salinity on AR7W during July 2-9, 2002, from Hudson 2002-032. The dashed lines trace layers of relative minimum potential temperature and relative maximum potential temperature as in Figure 3(a).

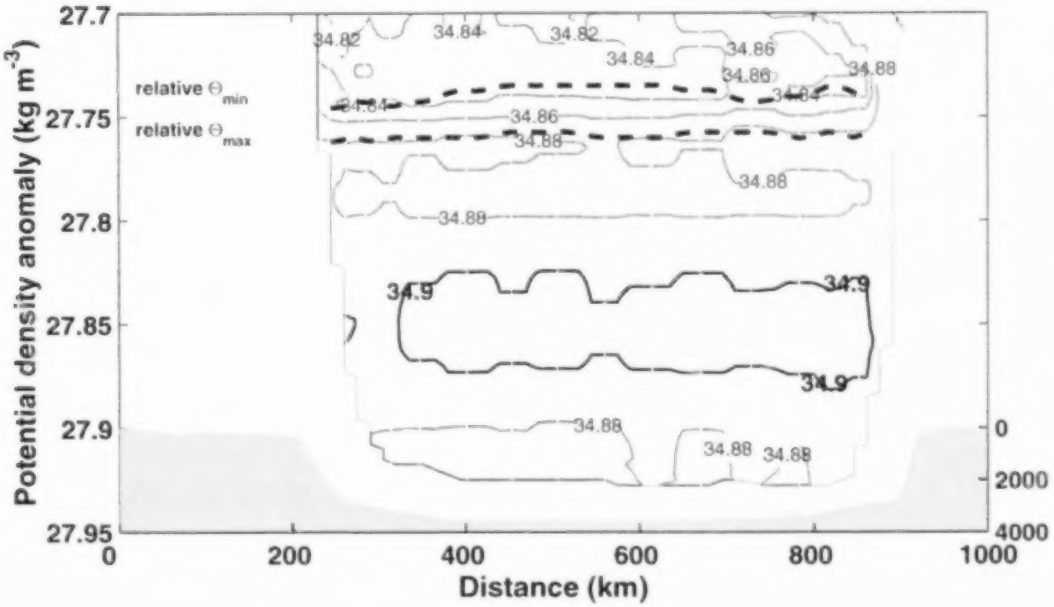

Fig. 4(b) Salinity on AR7W using potential density anomaly as the vertical coordinate for potential density anomalies greater than 27.7 kg·m^{-3} during July 2-9, 2002, from Hudson 2002-032 as in Figure 3(b).

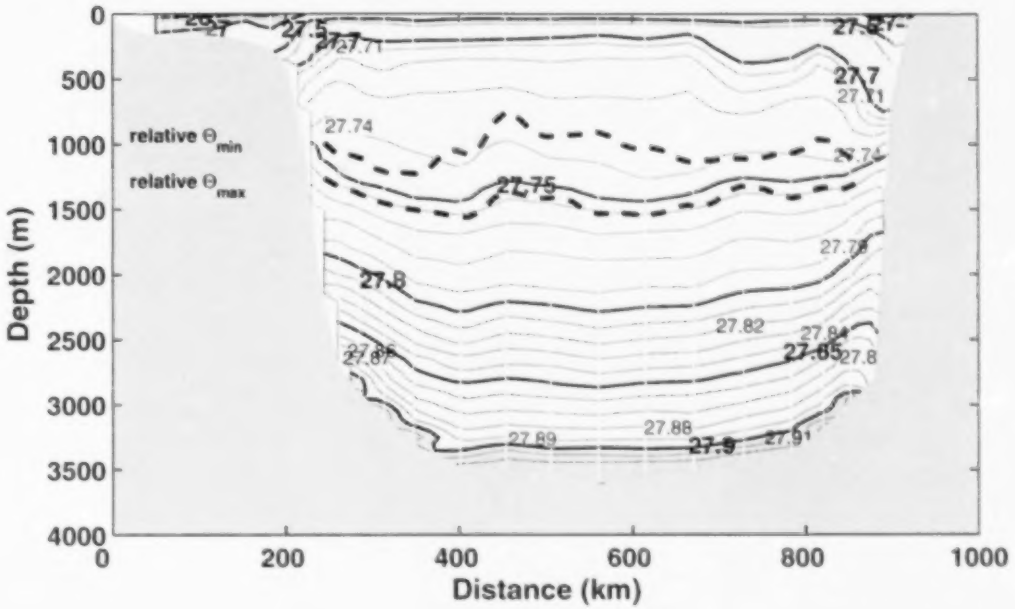

Fig. 5(a) Potential density anomaly (kg·m^{-3}) on AR7W during July 2-9, 2002, from Hudson 2002-032. The dashed lines trace layers of relative minimum potential temperature and relative maximum potential temperature as in Figure 3(a).

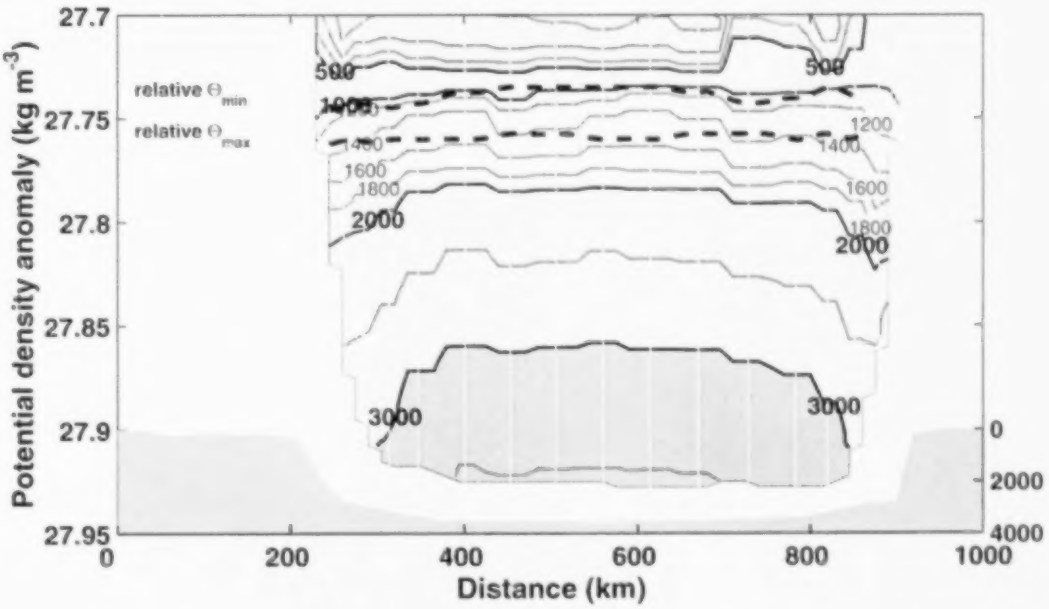

Fig. 5(b) Pressure (decibars) on AR7W using potential density anomaly as the vertical coordinate for potential density anomalies greater than 27.7 kg·m^{-3} during July 2-9, 2002, from Hudson 2002-032 as in Figure 3(b).

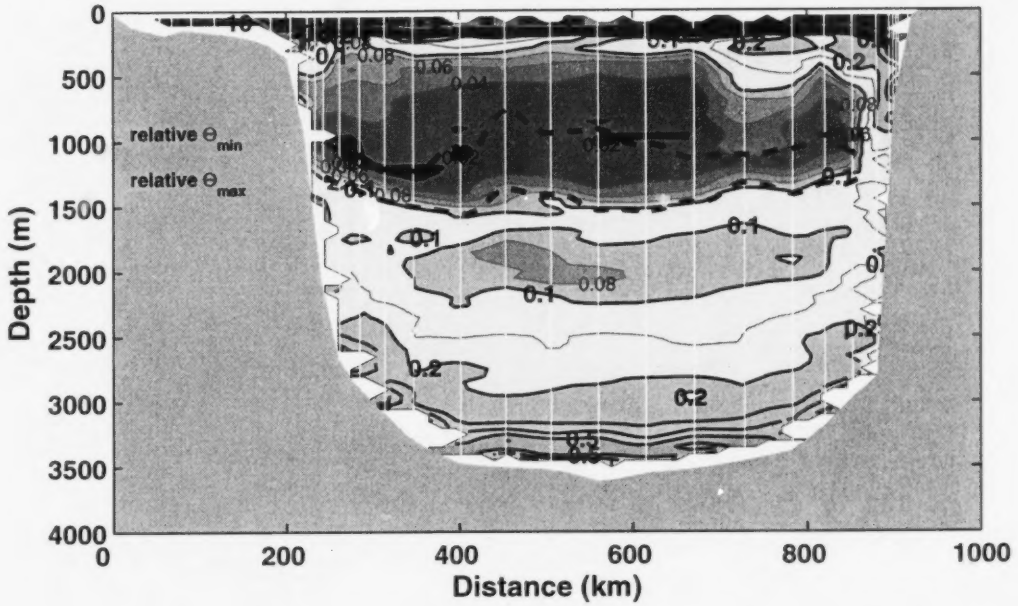

Fig. 6(a) Potential vorticity (10^{-10} $m^{-1} \cdot s^{-1}$) on AR7W during July 2-9, 2002, from Hudson 2002-032. The contoured field was produced from profiles that were smoothed in the vertical with a smoothing scale of 100m. The dashed lines trace layers of relative minimum potential temperature and relative maximum potential temperature as in Figure 3(a).

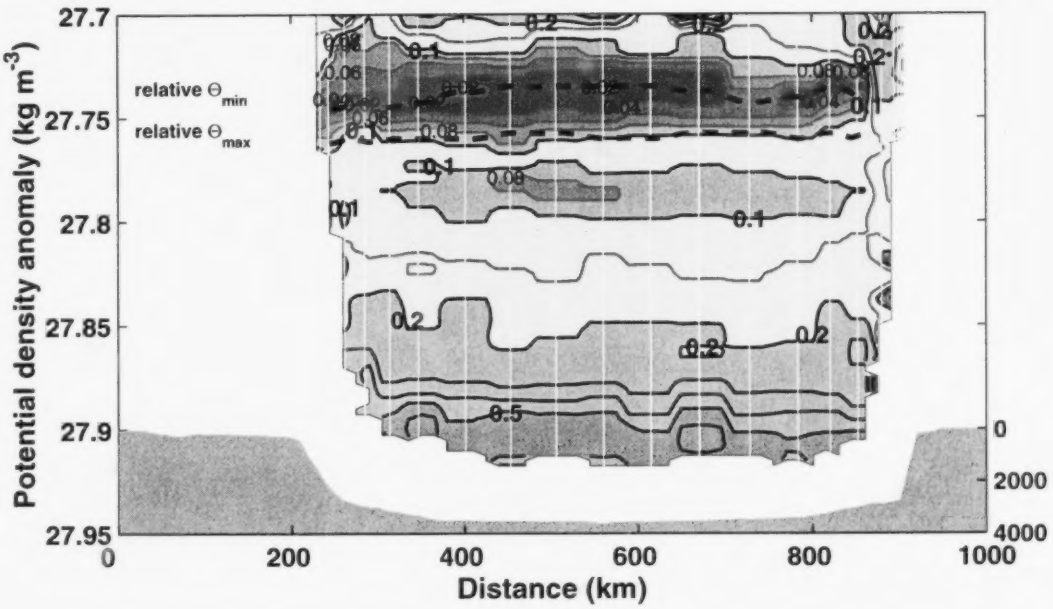

Fig. 6(b) Potential vorticity (10^{-10} $m^{-1} \cdot s^{-1}$) on AR7W using potential density anomaly as the vertical coordinate for potential density anomalies greater than 27.7 $kg \cdot m^{-3}$ during July 2-9, 2002, from Hudson 2002-032 as in Figure 3(b).

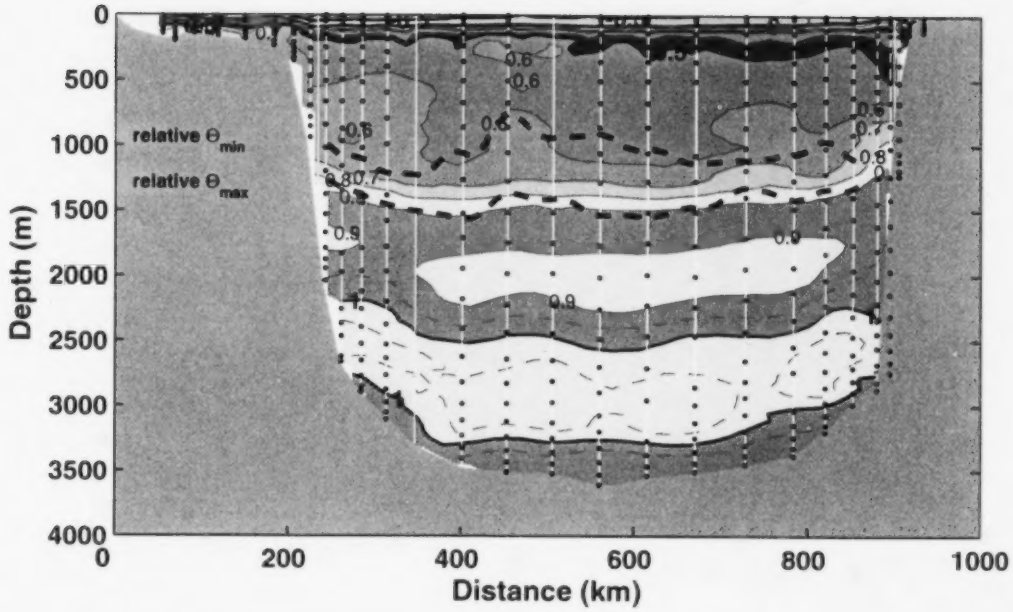

Fig. 7(a) Apparent oxygen utilisation (mL·L^{-1}) on AR7W during July 2-9, 2002, from Hudson 2002-032 bottle samples (indicated by dots). The dashed lines trace layers of relative minimum potential temperature and relative maximum potential temperature as in Figure 3(a).

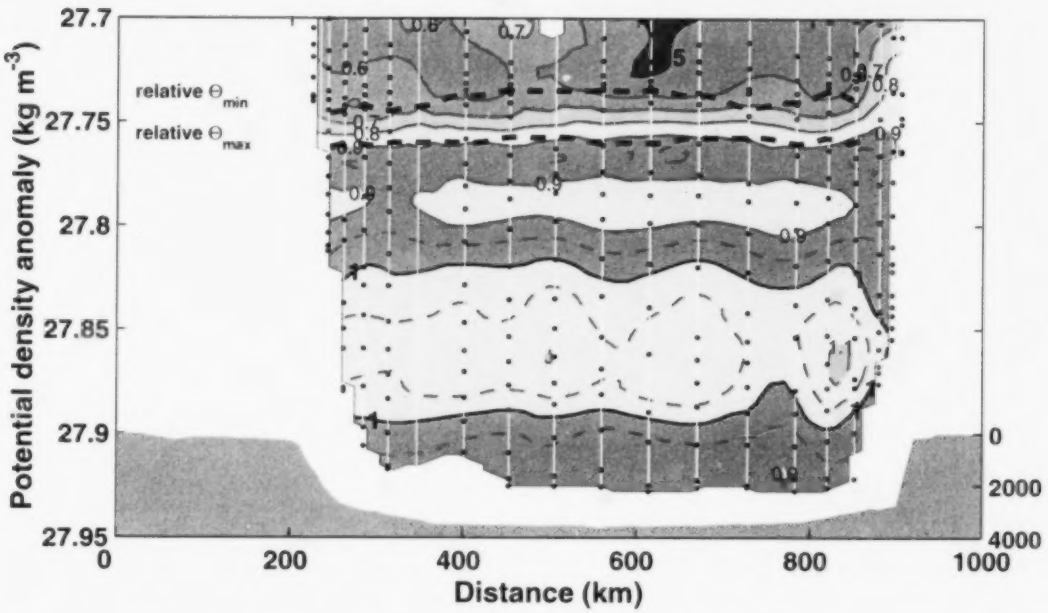

Fig. 7(b) Apparent oxygen utilisation (mL·L^{-1}) on AR7W using potential density anomaly as the vertical coordinate for potential density anomalies greater than 27.7 kg·m^{-3} during July 2-9, 2002, from Hudson 2002-032 as in Figure 3(b).

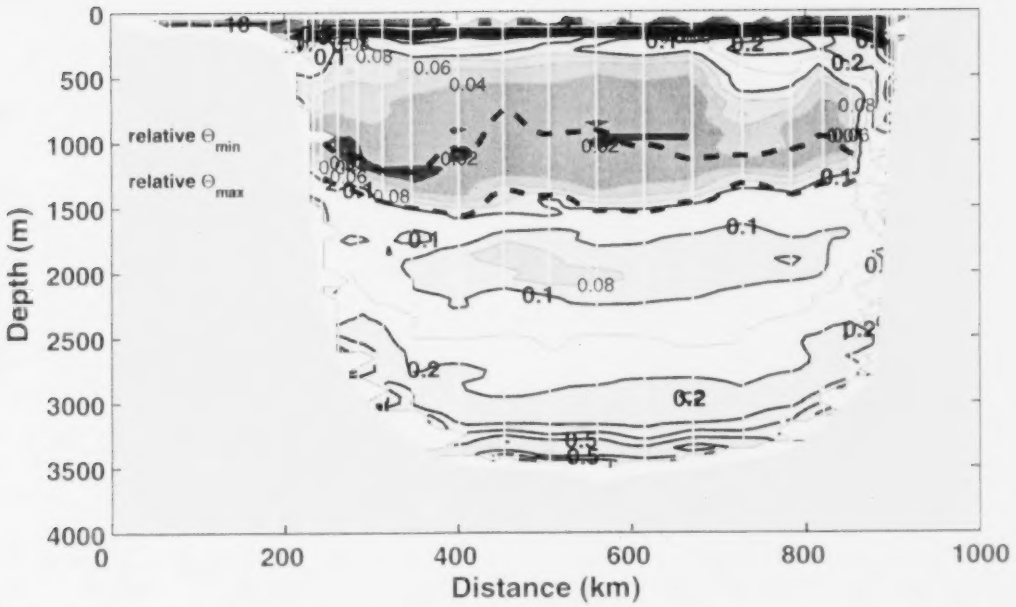

Fig. 6(a) Potential vorticity (10^{-10} $m^{-1} \cdot s^{-1}$) on AR7W during July 2-9, 2002, from Hudson 2002-032. The contoured field was produced from profiles that were smoothed in the vertical with a smoothing scale of 100m. The dashed lines trace layers of relative minimum potential temperature and relative maximum potential temperature as in Figure 3(a).

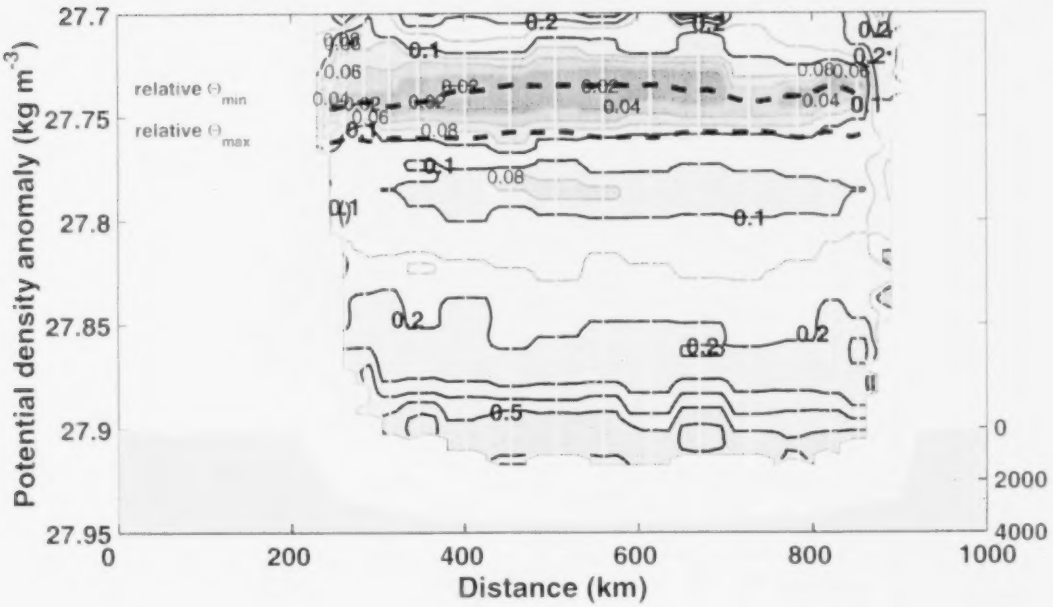

Fig. 6(b) Potential vorticity (10^{-10} $m^{-1} \cdot s^{-1}$) on AR7W using potential density anomaly as the vertical coordinate for potential density anomalies greater than 27.7 kg m^{-3} during July 2-9, 2002, from Hudson 2002-032 as in Figure 3(b).

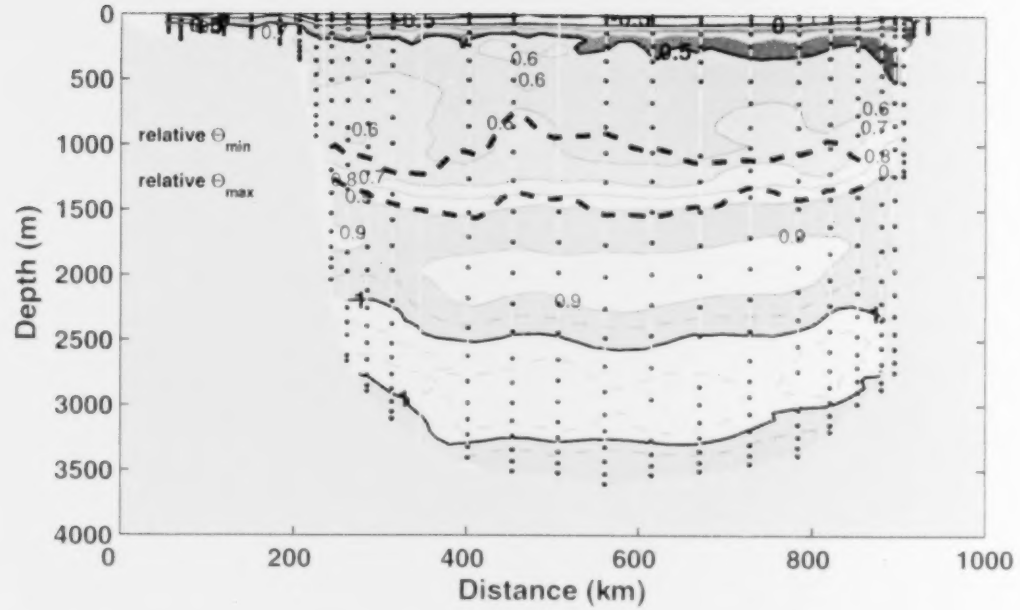

Fig. 7(a) Apparent oxygen utilisation (mL L^{-1}) on AR7W during July 2-9, 2002, from Hudson 2002-032 bottle samples (indicated by dots). The dashed lines trace layers of relative minimum potential temperature and relative maximum potential temperature as in Figure 3(a).

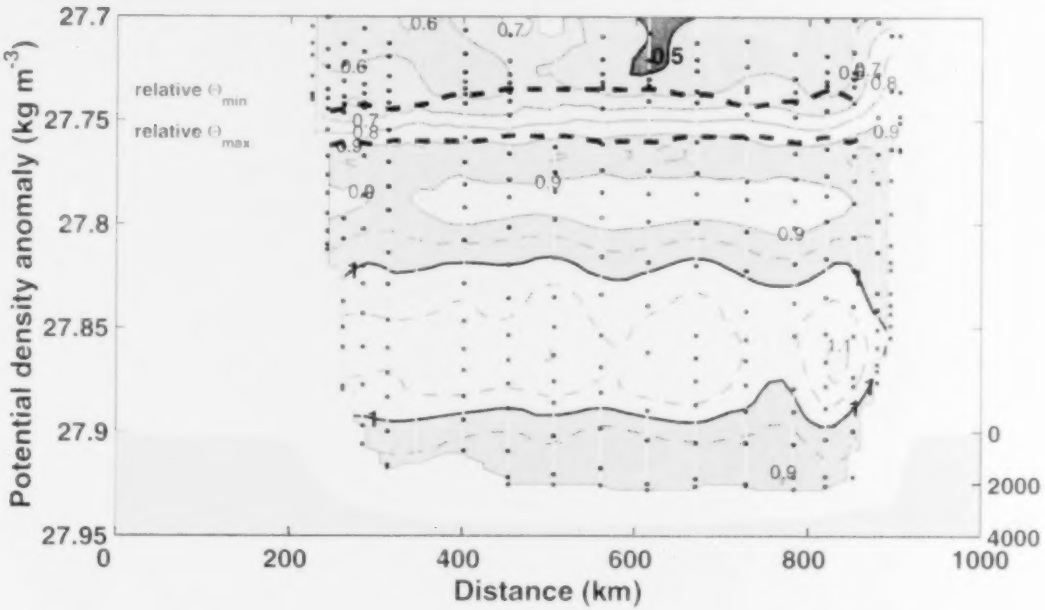

Fig. 7(b) Apparent oxygen utilisation (mL L^{-1}) on AR7W using potential density anomaly as the vertical coordinate for potential density anomalies greater than 27.7 kg m^{-3} during July 2-9, 2002, from Hudson 2002-032 as in Figure 3(b).

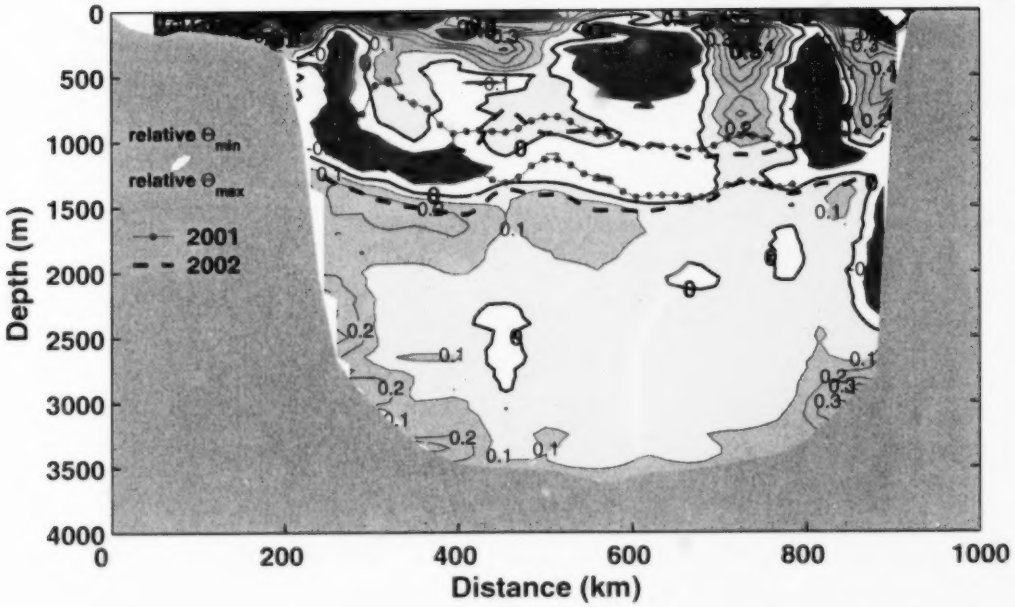

Fig. 8(a) Potential temperature change (°C) on AR7W from June 2001 (Hudson 2001-022) to July 2002 (Hudson 2002-032). The dashed and dotted lines trace layers of relative minimum potential temperature and relative maximum potential temperature for the two years.

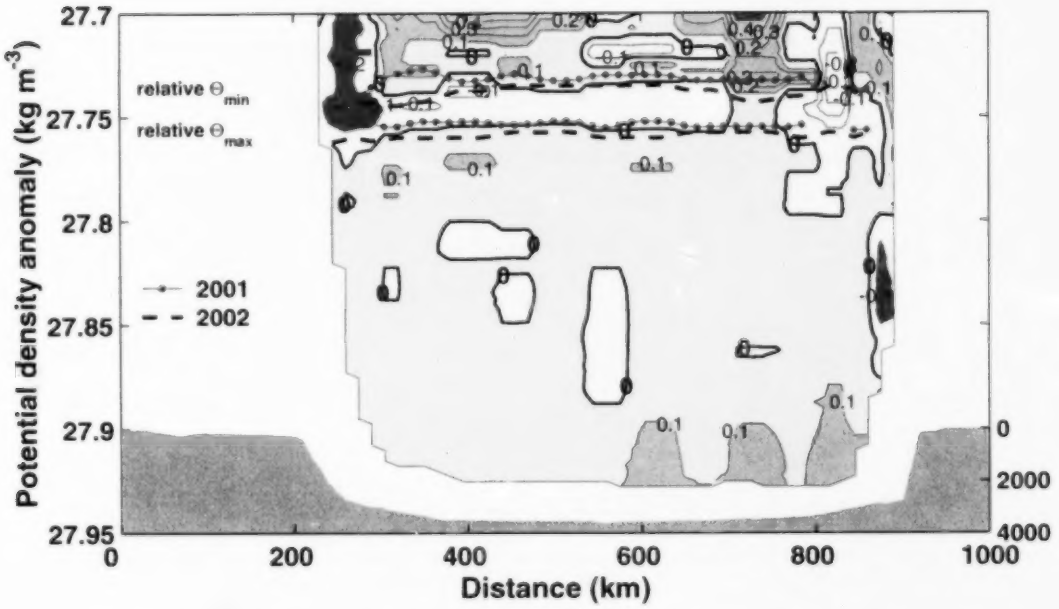

Fig. 8(b) Potential temperature change (°C) on AR7W from June 2001 to July 2002 using potential density anomaly as the vertical coordinate for potential density anomalies greater than 27.7 kg·m^{-3}. The dashed and dotted lines trace layers of relative minimum and maximum potential temperature as in Figure 8(a). An overlay shows the section bathymetry (m). The scale for the bathymetry is at lower right.

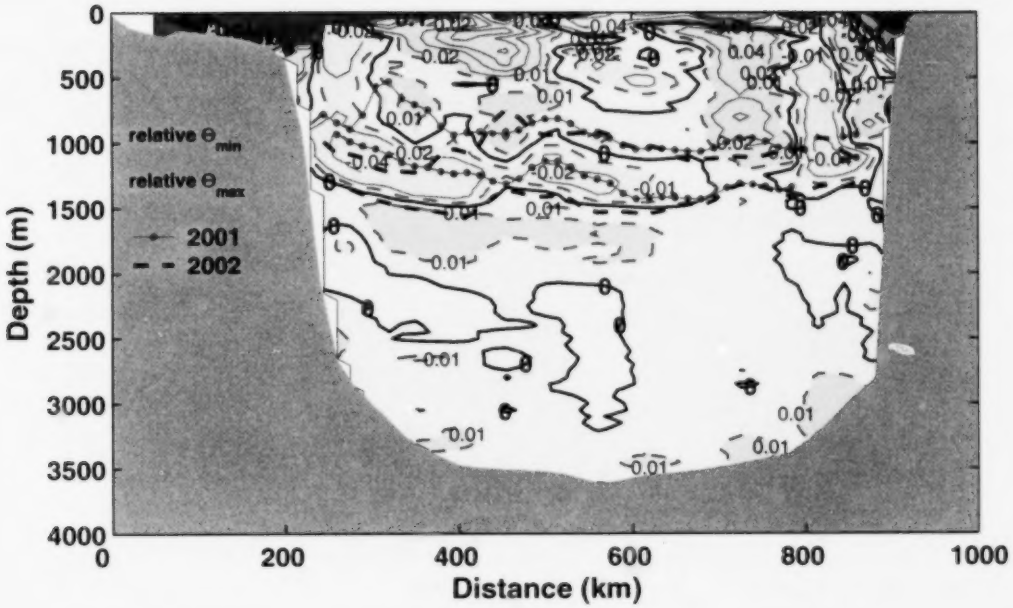

Fig. 9(a) Salinity change on AR7W from June 2001 to July 2002. The dashed and dotted lines trace layers of relative minimum potential temperature and relative maximum potential temperature as in Figure 8(a).

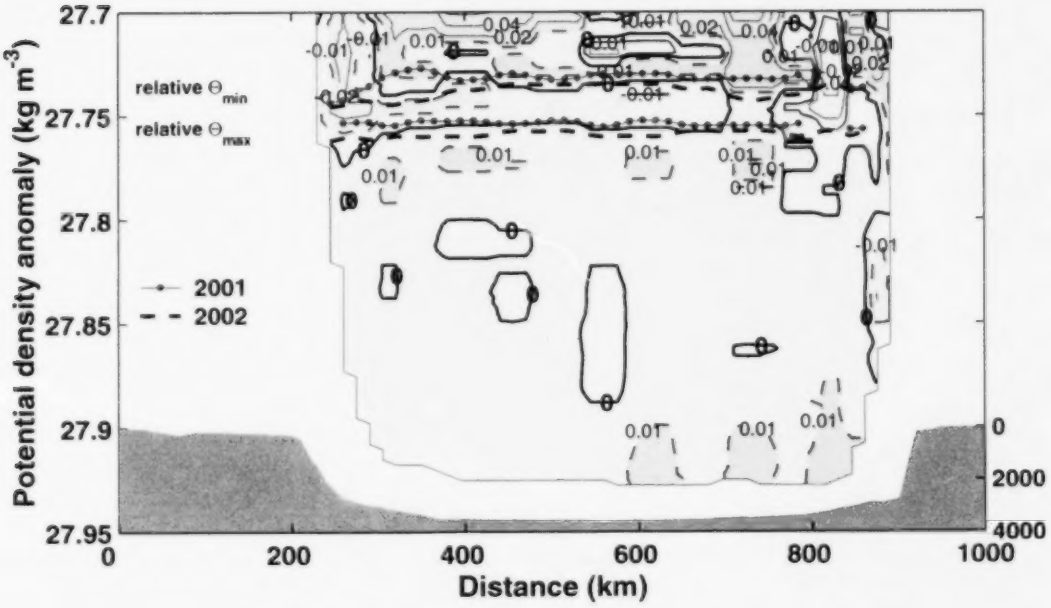

Fig. 9(b) Salinity change on AR7W from June 2001 to July 2002 using potential density anomaly as the vertical coordinate as in Figure 8(b).

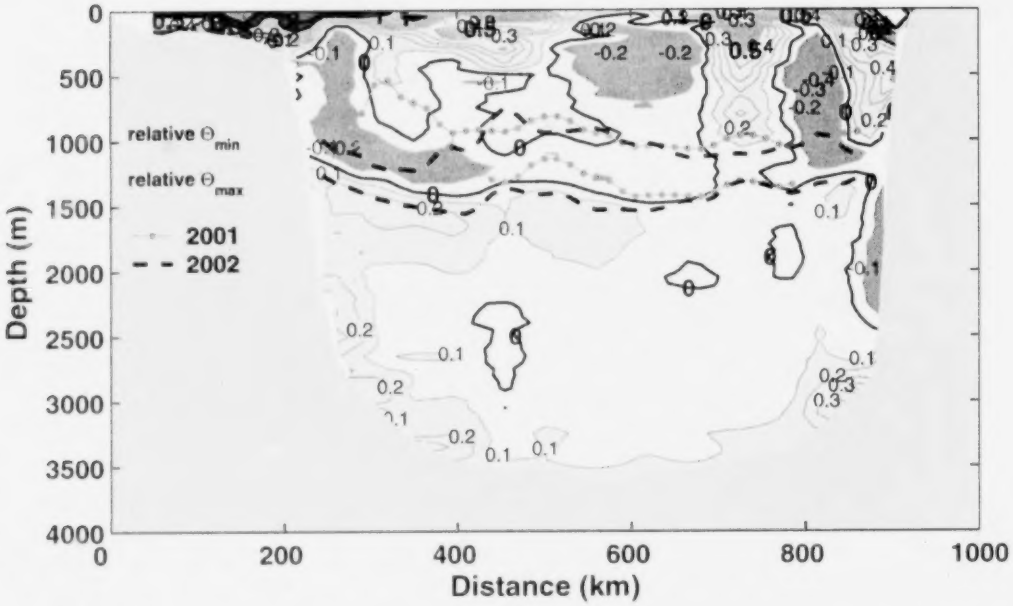

Fig. 8(a) Potential temperature change (°C) on AR7W from June 2001 (Hudson 2001-022) to July 2002 (Hudson 2002-032). The dashed and dotted lines trace layers of relative minimum potential temperature and relative maximum potential temperature for the two years.

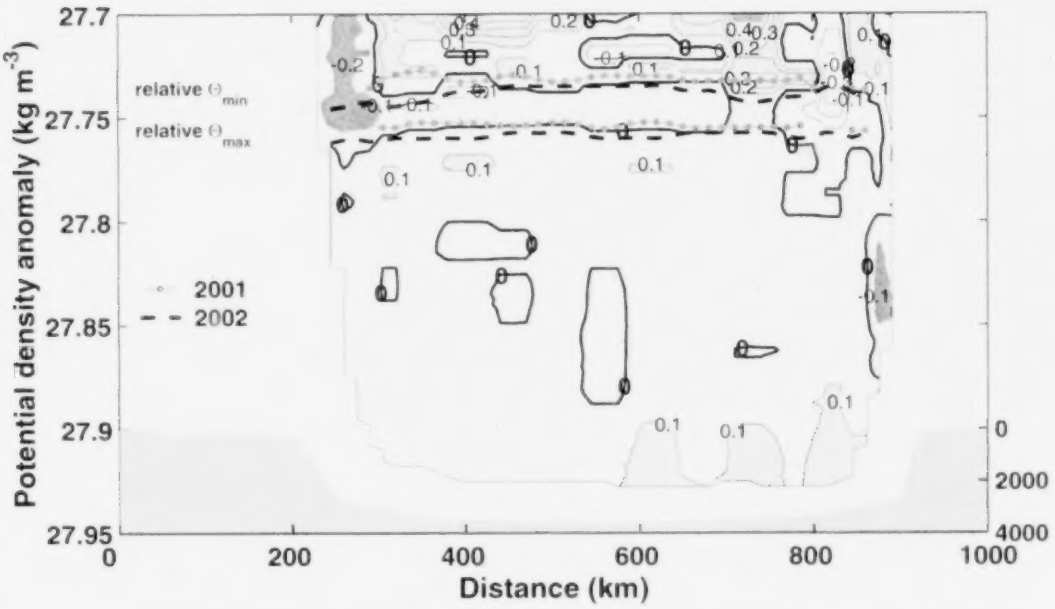

Fig. 8(b) Potential temperature change (°C) on AR7W from June 2001 to July 2002 using potential density anomaly as the vertical coordinate for potential density anomalies greater than 27.7 kg m^{-3}. The dashed and dotted lines trace layers of relative minimum and maximum potential temperature as in Figure 8(a). An overlay shows the section bathymetry (m). The scale for the bathymetry is at lower right.

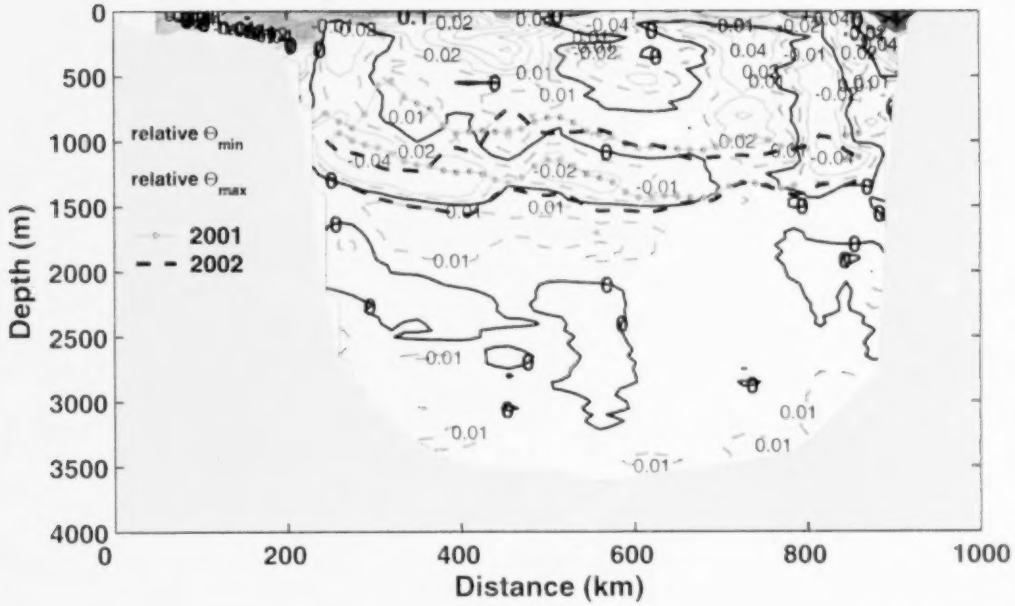

Fig. 9(a) Salinity change on AR7W from June 2001 to July 2002. The dashed and dotted lines trace layers of relative minimum potential temperature and relative maximum potential temperature as in Figure 8(a).

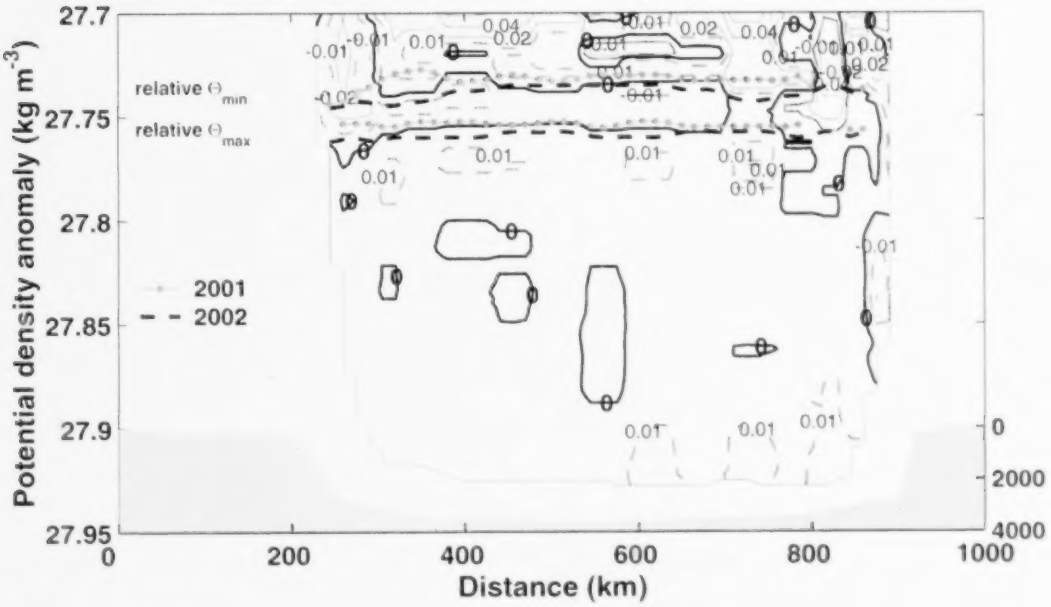

Fig. 9(b) Salinity change on AR7W from June 2001 to July 2002 using potential density anomaly as the vertical coordinate as in Figure 8(b).

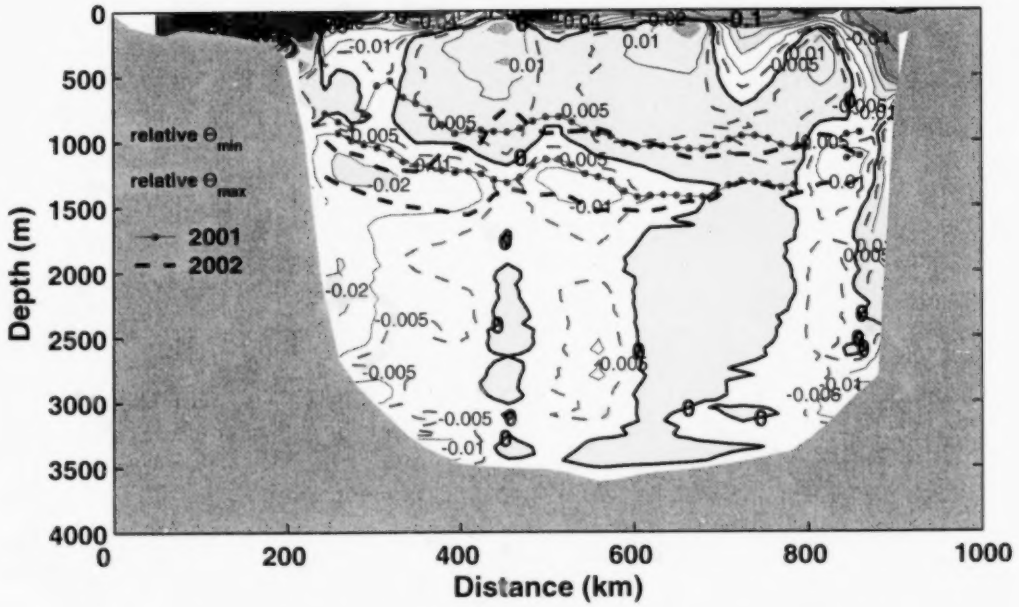

Fig. 10(a) Potential density change (kg·m^{-3}) on AR7W from June 2001 to July 2002. The dashed and dotted lines trace layers of relative minimum potential temperature and relative maximum potential temperature as in Figure 8(a).

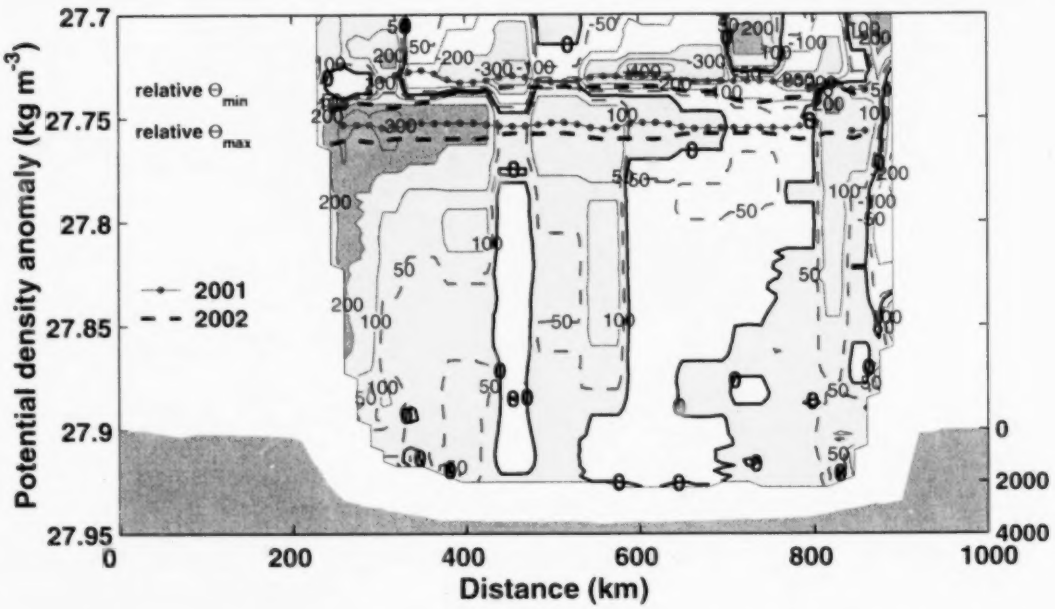

Fig. 10(b) Pressure change (dbar) on AR7W from June 2001 to July 2002 using potential density anomaly as the vertical coordinate as in Figure 8(b).

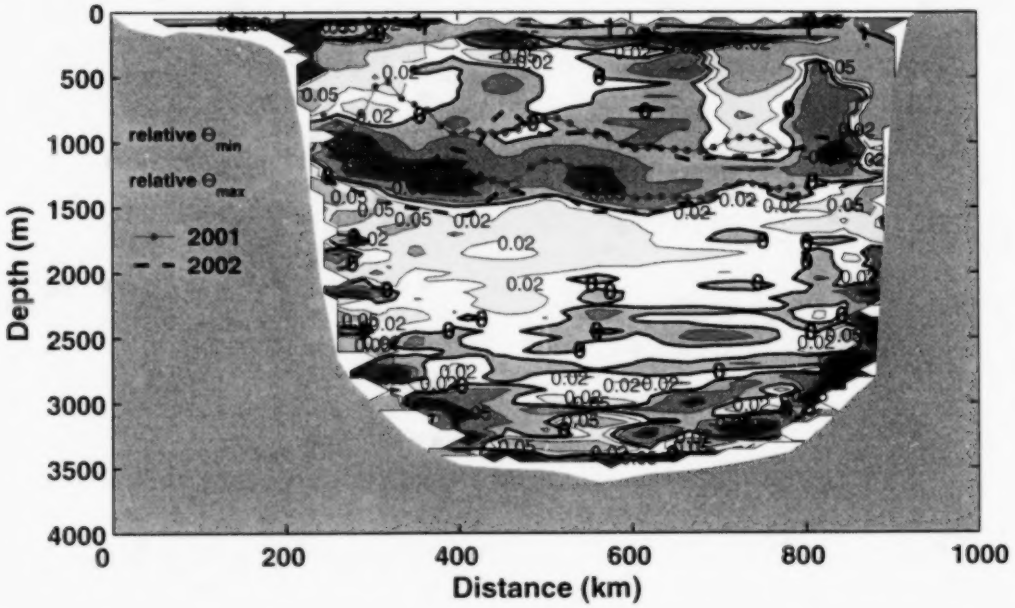

Fig. 11(a) Potential vorticity change (10^{-10} $m^{-1} \cdot s^{-1}$) on AR7W from June 2001 to July 2002. The dashed and dotted lines trace layers of relative minimum potential temperature and relative maximum potential temperature as in Figure 8(a).

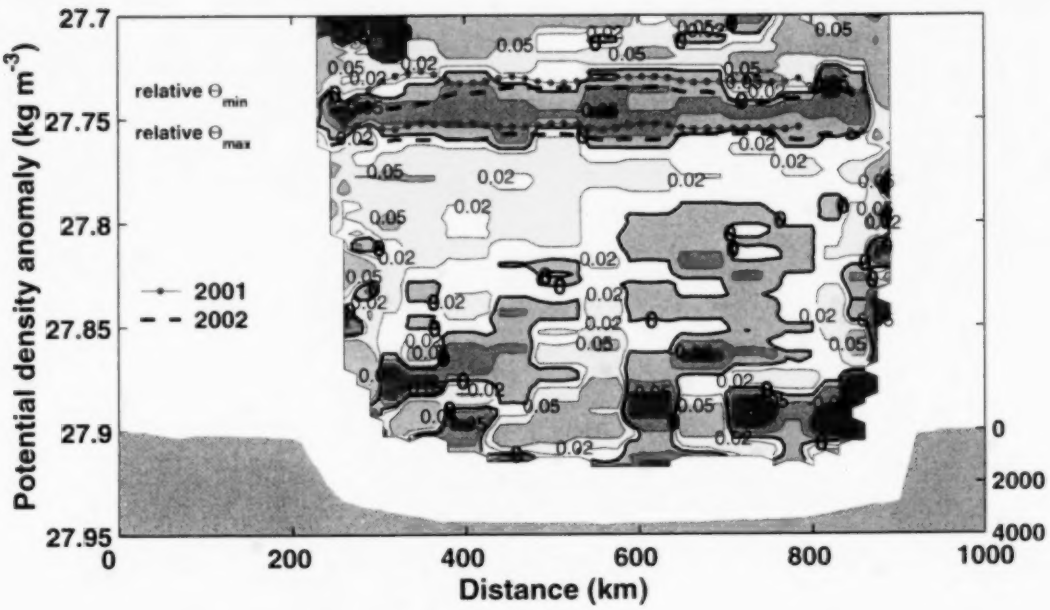

Fig. 11(b) Potential vorticity change (10^{-10} $m^{-1} \cdot s^{-1}$) on AR7W from June 2001 to July 2002 using potential density anomaly as the vertical coordinate as in Figure 8(b).

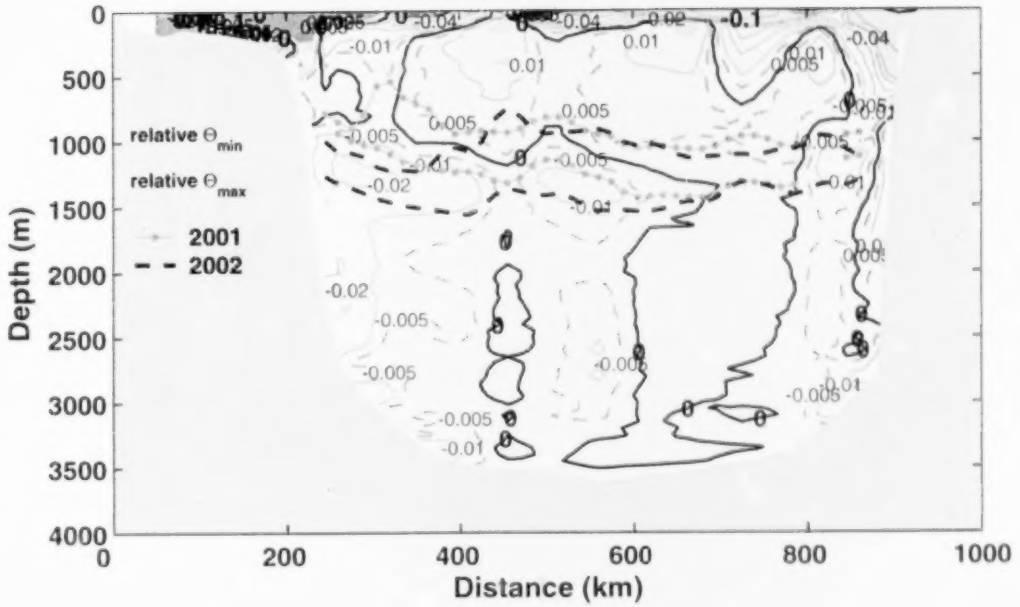

Fig. 10(a) Potential density change (kg·m^{-3}) on AR7W from June 2001 to July 2002. The dashed and dotted lines trace layers of relative minimum potential temperature and relative maximum potential temperature as in Figure 8(a).

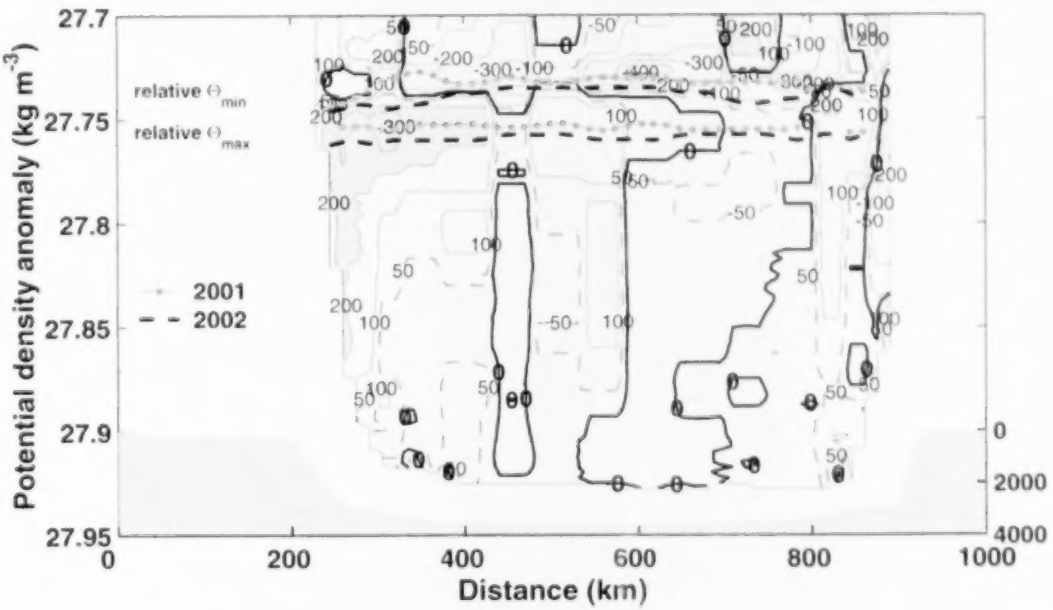

Fig. 10(b) Pressure change (dbar) on AR7W from June 2001 to July 2002 using potential density anomaly as the vertical coordinate as in Figure 8(b).

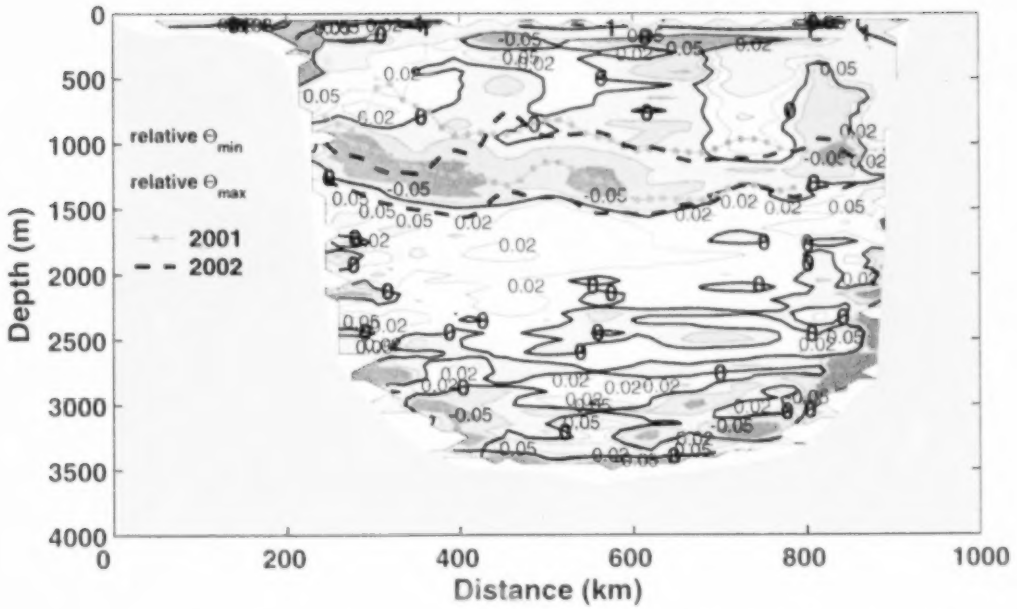

Fig. 11(a) Potential vorticity change (10^{-10} $m^{-1} \cdot s^{-1}$) on AR7W from June 2001 to July 2002. The dashed and dotted lines trace layers of relative minimum potential temperature and relative maximum potential temperature as in Figure 8(a).

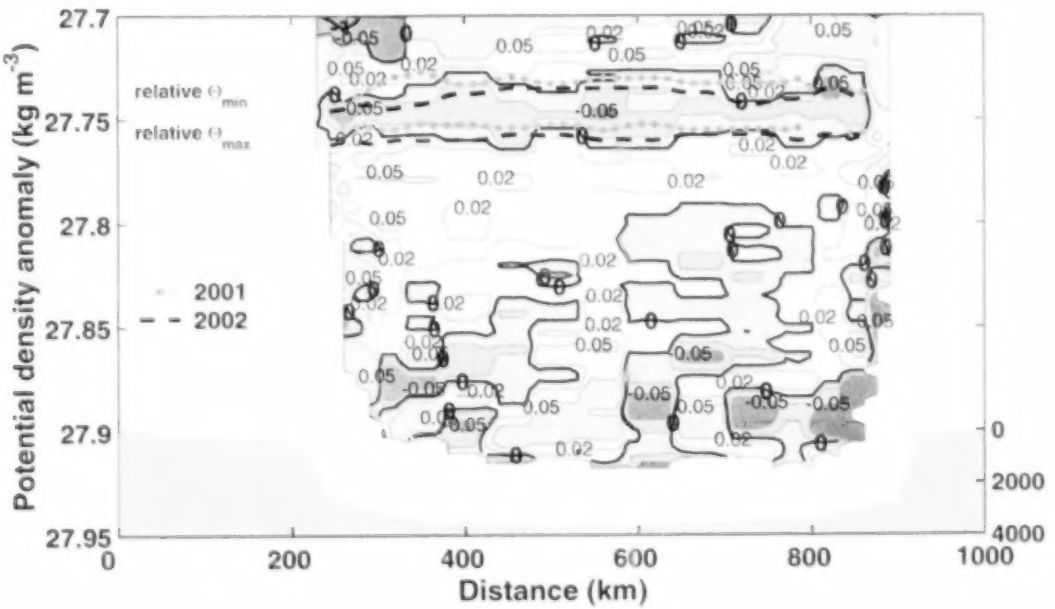

Fig. 11(b) Potential vorticity change (10^{-10} $m^{-1} \cdot s^{-1}$) on AR7W from June 2001 to July 2002 using potential density anomaly as the vertical coordinate as in Figure 8(b).

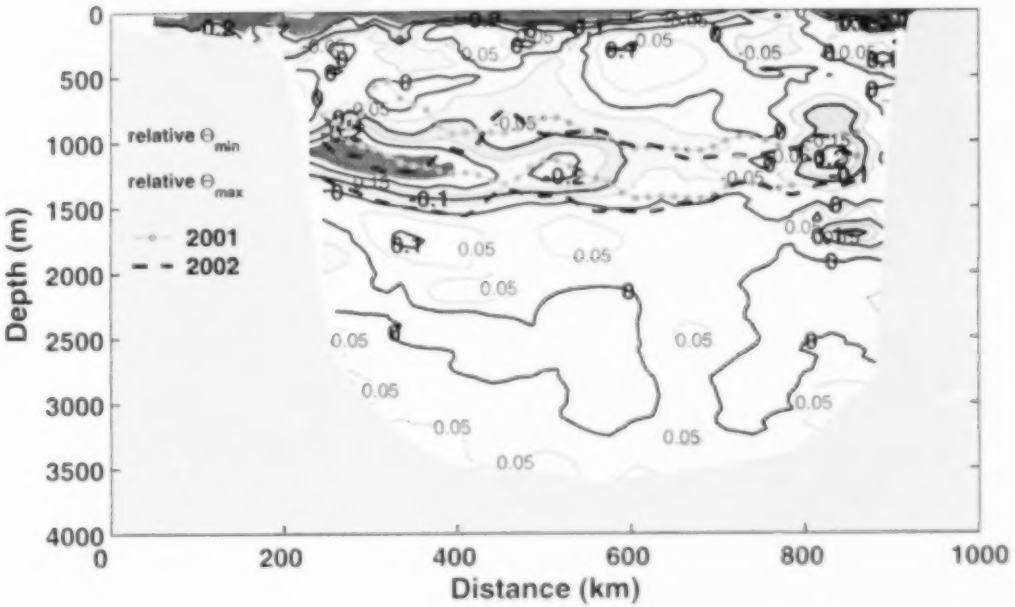

Fig. 12(a) Apparent oxygen utilisation change (mL·L^{-1}) on AR7W from June 2001 to July 2002 using bottle samples. The dashed and dotted lines trace layers of relative minimum potential temperature and relative maximum potential temperature as in Figure 8(a).

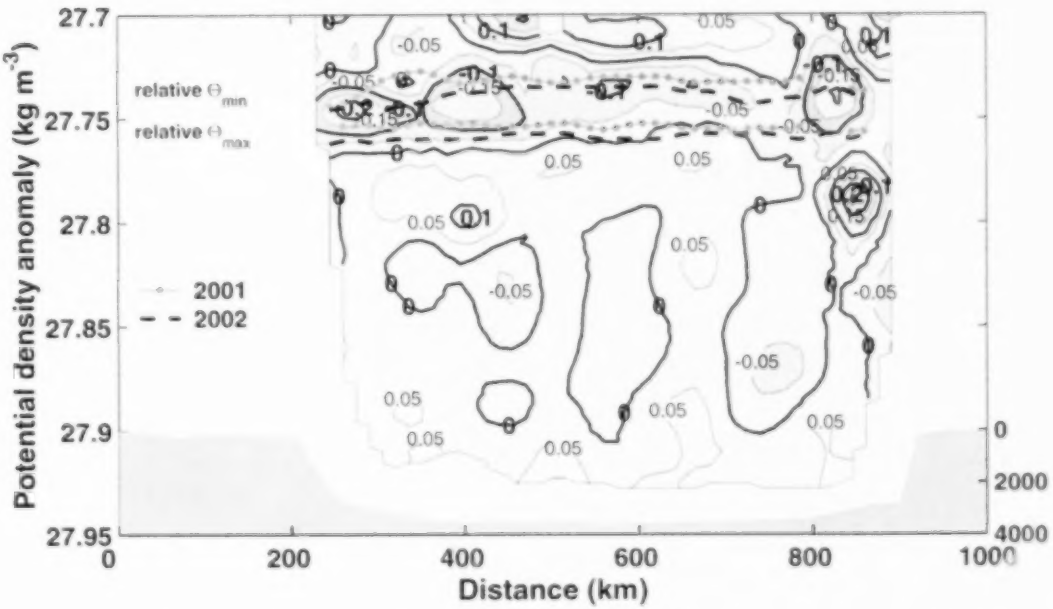

Fig. 12(b) Apparent oxygen utilisation change (mL·L^{-1}) on AR7W from June 2001 to July 2002 using potential density anomaly as the vertical coordinate as in Figure 8(b).

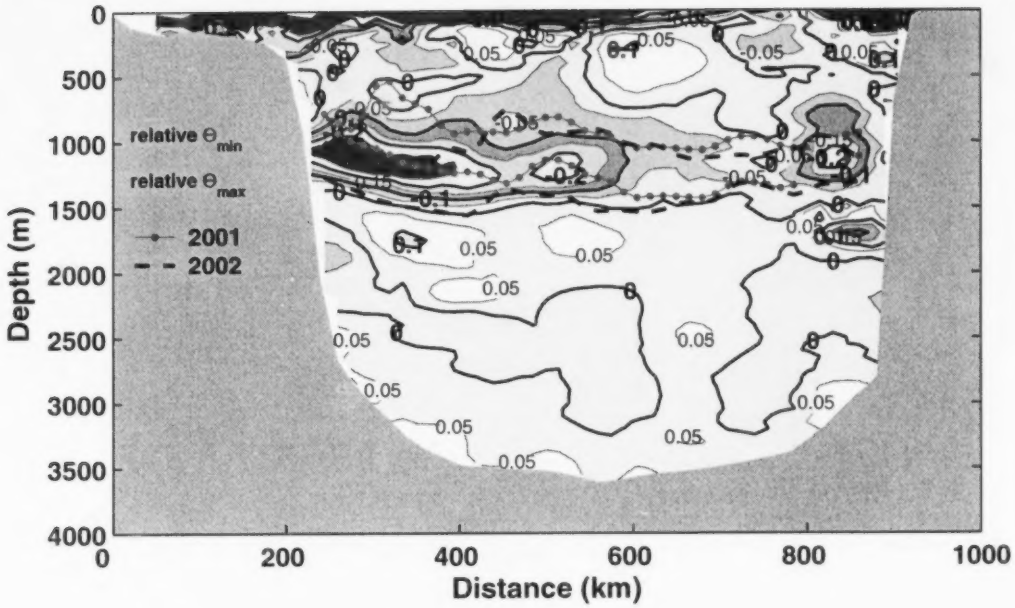

Fig. 12(a) Apparent oxygen utilisation change (mL·L^{-1}) on AR7W from June 2001 to July 2002 using bottle samples. The dashed and dotted lines trace layers of relative minimum potential temperature and relative maximum potential temperature as in Figure 8(a).

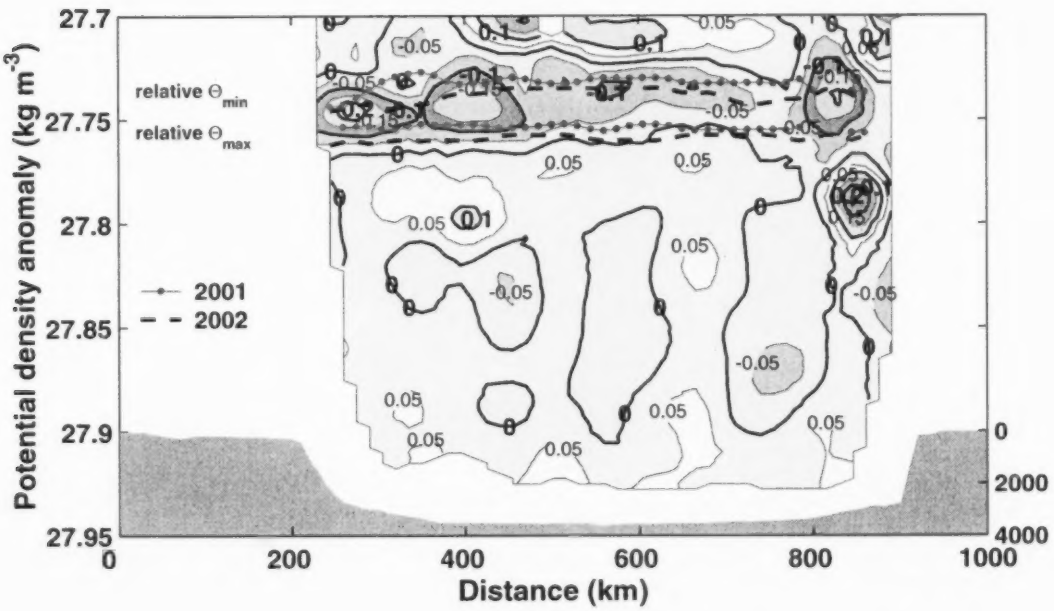

Fig. 12(b) Apparent oxygen utilisation change (mL·L^{-1}) on AR7W from June 2001 to July 2002 using potential density anomaly as the vertical coordinate as in Figure 8(b).

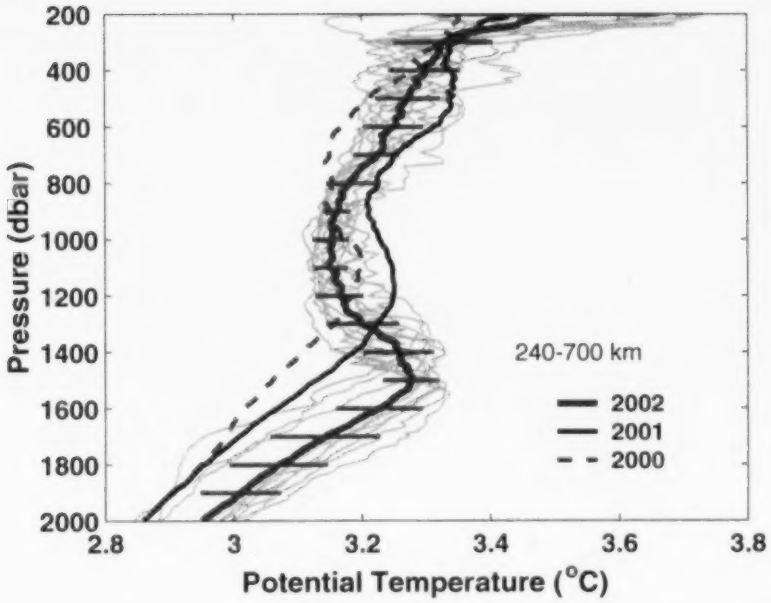

Fig. 13(a) Potential temperature averaged on pressure surfaces for distances in the range 240-700km for 2002, 2001, and 2000 using pressure as the vertical coordinate. Individual profiles and selected standard deviations for 2002 are plotted in the background.

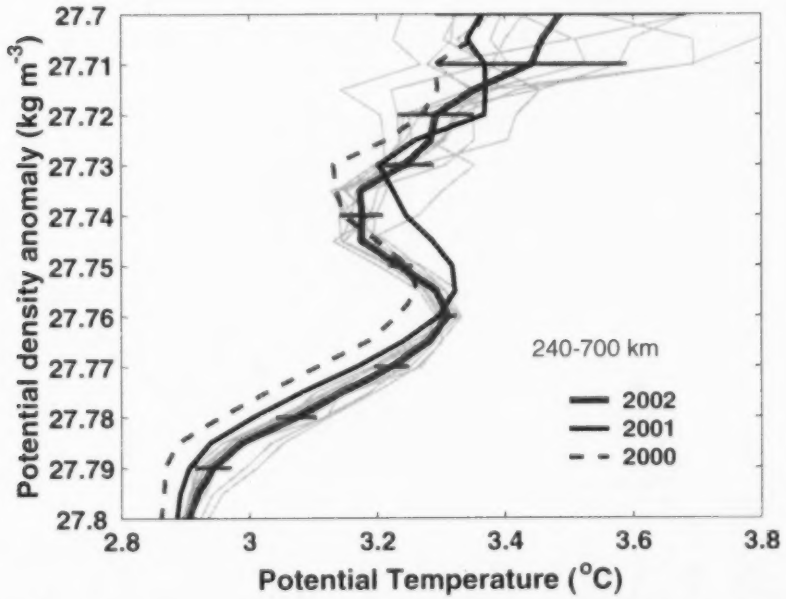

Fig. 13(b) Potential temperature averaged on potential density for distances in the range 240-700km for 2002, 2001, and 2000 using potential density anomaly as the vertical coordinate for potential density anomalies between 27.7 and 27.8 kg·m^{-3}. Individual profiles and selected standard deviations for 2002 are plotted in the background.

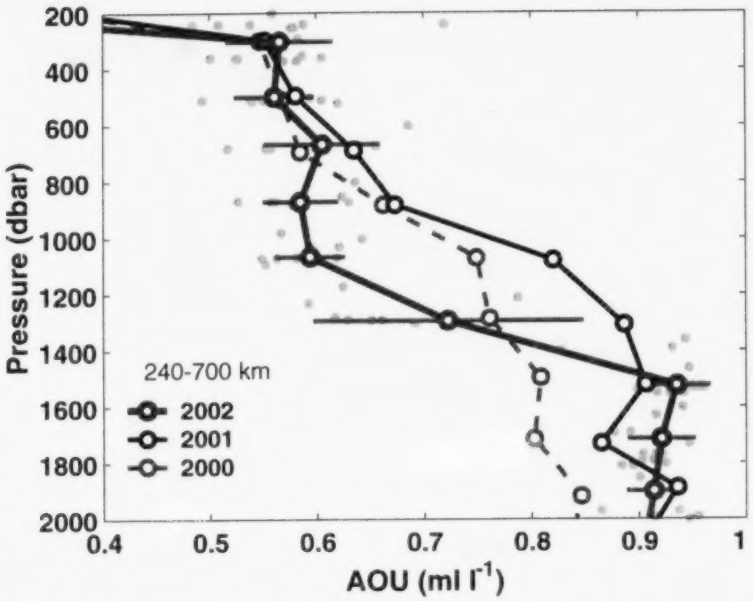

Fig. 14(a) Apparent oxygen utilisation (AOU) from discrete bottle values averaged in 200-dbar bins for distances in the range 240-700km using pressure as the vertical coordinate for 2002, 2001, and 2000. Individual values and standard deviations for 2002 are plotted in the background.

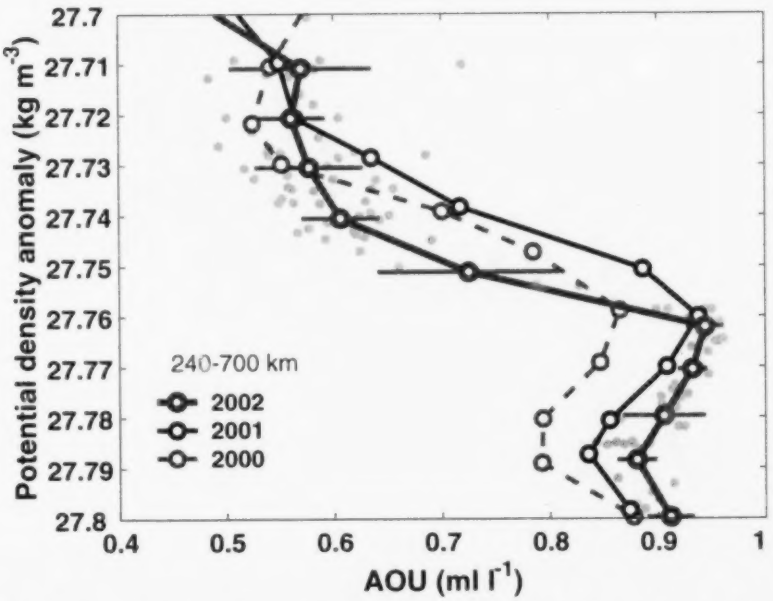

Fig. 14(b) Apparent oxygen utilisation (AOU) from discrete bottle values averaged in 0.01 kg·m-3 potential density bins as a function of potential density anomaly for distances in the range 240-700km for 2002, 2001, and 2000 using potential density anomaly between 27.7 and 27.8 kg·m^{-3} as the vertical coordinate. Individual values and standard deviations for 2002 are plotted in the background.

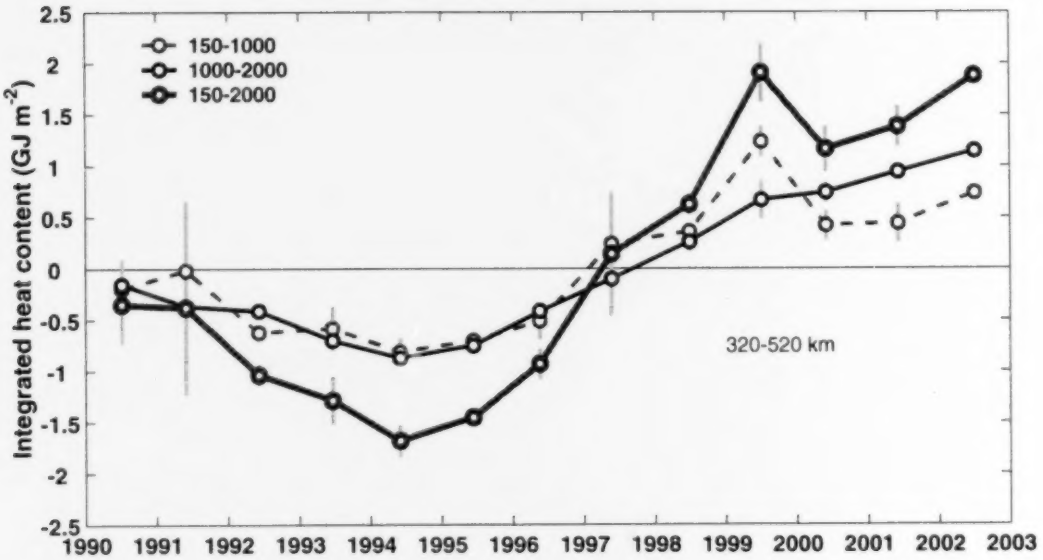

Fig. 15(a) Heat content from spring AR7W occupations averaged over stations in the distance range 320-520km as a function of median station time. Integrals over 150-1000m and 1000-2000m and their sum are shown. The average heat content in the respective depth ranges for the 13 spring occupations has been removed. The error bars are standard deviations.

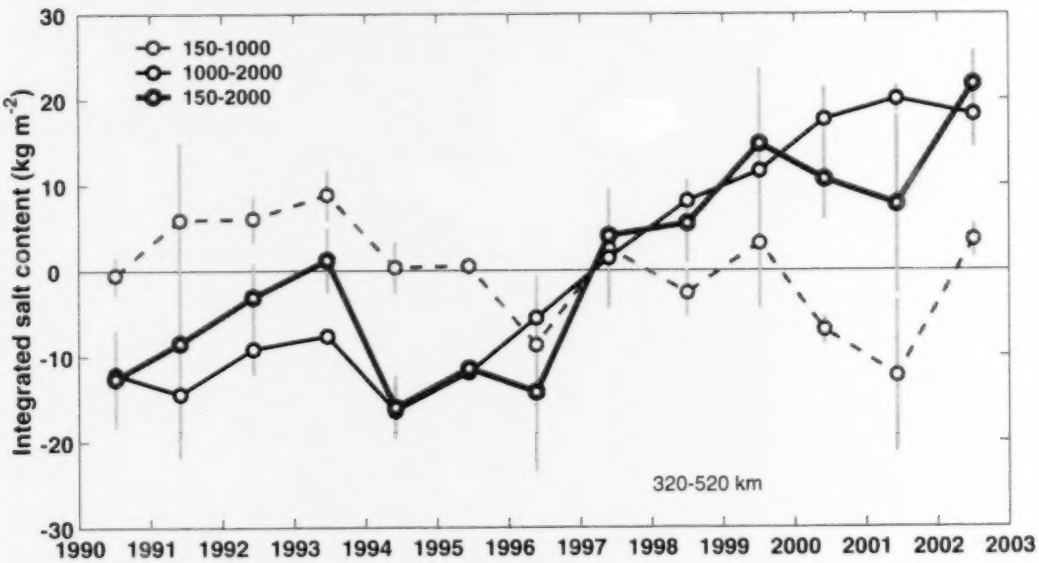

Fig. 15(b) Salt content from spring AR7W occupations averaged over stations in the distance range 320-520km for different depth layers as a function of median station time as in Fig. 15(a).

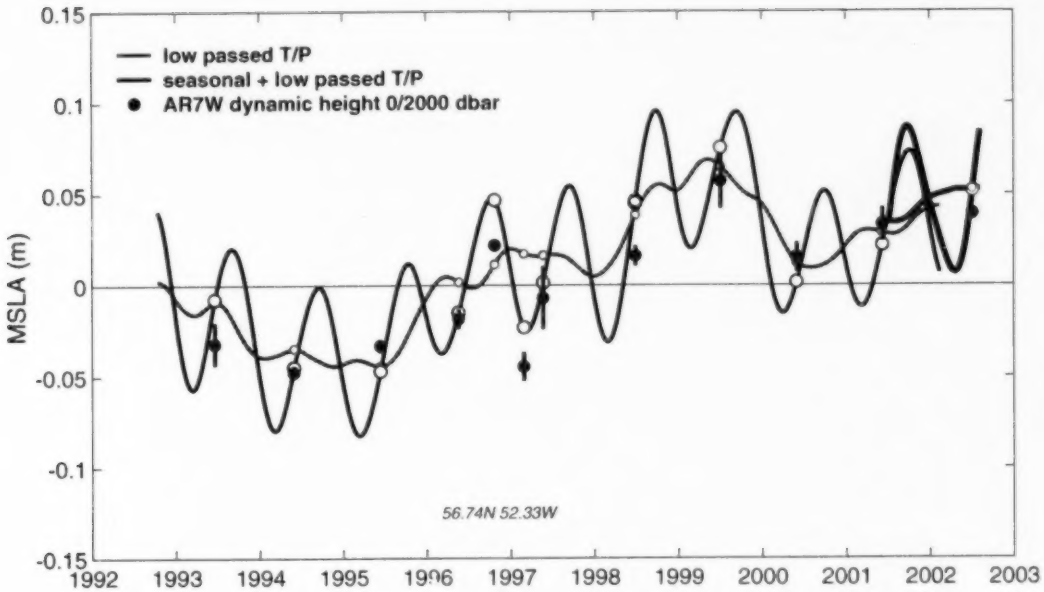

Fig. 16 TOPEX/POSEIDON sea level anomaly near the Bravo mooring site. Low-passed sea-level changes are shown with and without the seasonal cycle. The filled circles show the 0-2000 dbar geopotential height from AR7W occupations averaged over stations in the 320-520km distance range, with associated standard deviations. The open circles mark T/P sea level including seasonal changes at the same times. Most of the analysis is based on the AVISO MSLA product. The last, partly overlapping part of the analysis (indicated by slightly heavier lines) is based on crossover time series for Tracks 243 and 098.

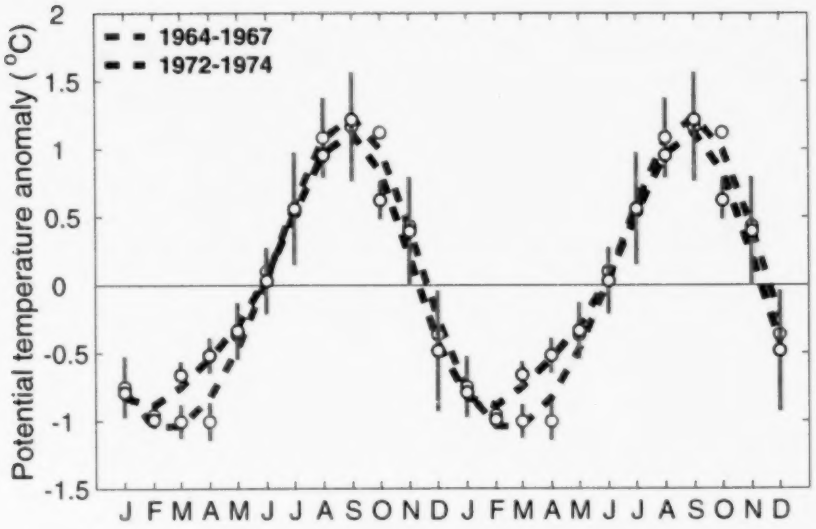

Fig. A1 Annual cycles in 0-150m depth-averaged potential temperature relative to the period means from OWS Bravo for January 1964 - December 1967 and June 1972 - May 1974, repeated for two annual cycles. Means of monthly means (open circles) are plotted against mid-month date. The error bars are standard deviations of the monthly means for the two periods. The dashed curves are least-squares fits of annual and semi-annual harmonics.

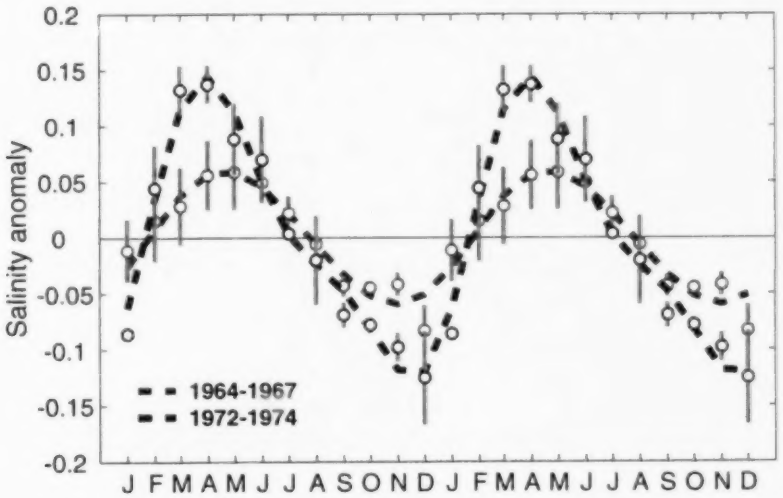

Fig. A2 Annual cycles in 0-150m depth-averaged salinity relative to the period means from OWS Bravo as in Fig. A1.

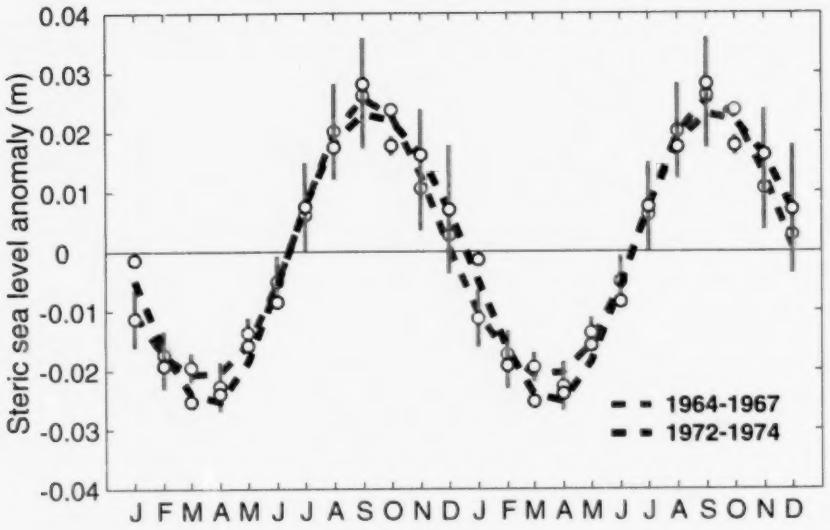

Fig. A3 Annual cycles in 0-150m steric sea level from OWS Bravo as in Fig. A1.